J Nonlinear Sci (2013) 23:205–239
DOI 10.1007/s00332-012-9149-y

Journal of Nonlinear Science

Breathers for the Discrete Nonlinear Schrödinger Equation with Nonlinear Hopping

N.I. Karachalios · B. Sánchez-Rey · P.G. Kevrekidis · J. Cuevas

Received: 24 March 2011 / Accepted: 6 September 2012 / Published online: 13 December 2012

Abstract We discuss the existence of breathers and lower bounds on their power, in nonlinear Schrödinger lattices with nonlinear hopping. Our methods extend from a simple variational approach to fixed-point arguments, deriving lower bounds for the power which can serve as a threshold for the existence of breather solutions. Qualitatively, the theoretical results justify non-existence of breathers below the prescribed lower bounds of the power which depend on the dimension, the parameters of the lattice as well as of the frequency of breathers. In the case of supercritical power nonlinearities we investigate the interplay of these estimates with the optimal constant of the discrete interpolation inequality. Improvements of the general estimates, taking into account the localization of the true breather solutions are derived. Numerical studies in the one-dimensional lattice corroborate the theoretical bounds and illustrate that in certain parameter regimes of physical significance, the estimates can serve as accurate predictors of the breather power and its dependence on the various system parameters.

Communicated by P. Newton.

N.I. Karachalios (✉)
Department of Mathematics, University of the Aegean, Karlovassi, 83200 Samos, Greece
e-mail: karan@aegean.gr

B. Sánchez-Rey · J. Cuevas
Grupo de Física No Lineal, Departamento de Física Aplicada I, Universidad de Sevilla, C/Virgen de Africa, 7, 41011 Sevilla, Spain

P.G. Kevrekidis
Department of Mathematics and Statistics, University of Massachusetts, Lederle Graduate Research Tower, Amherst, MA 01003-9305, USA

Keywords Discrete Nonlinear Schrödinger equation · Variational methods · Fixed-point methods · Nonlinear hopping · Localization length · Breathers · Solitons · Numerical results

Mathematics Subject Classification 37L60 · 34A33 · 34L40 · 35C07 · 35Q55 · 37K40

1 Introduction

The discrete nonlinear Schrödinger (DNLS) model constitutes a ubiquitous example of a nonlinear dynamical lattice with a wide range of applications, extending from the nonlinear optics of fabricated AlGaAs waveguide arrays as in Christodoulides et al. (2003), Kivshar and Agrawal (2003), Lederer et al. (2008), to the atomic physics of Bose–Einstein condensates in sufficiently deep optical lattices analyzed in Konotop and Brazhnyi (2004), Morsch and Oberthaler (2006), Kevrekidis and Frantzeskakis (2004), Kevrekidis et al. (2008). Partly also due to these applications, the DNLS has been a focal point of numerous mathematical/computational investigations in its own right, a number of which has been summarized in Kevrekidis et al. (2001), Eilbeck and Johansson (2003), Kevrekidis (2009), Flach and Willis (1998), Hennig and Tsironis (1999), Flach and Gorbach (2008) and is related to models used in numerous other settings including micromechanical cantilever arrays (Sato et al. 2006) and DNA breathing dynamics (Peyrard 2004), among others.

In this work we consider a variant of the DNLS equation of the following form:

$$\mathrm{i}\dot{\psi}_n + \epsilon(\Delta_d\psi)_n + \alpha\psi_n \sum_{j=1}^{N}(\mathcal{T}_j\psi)_{n\in\mathbb{Z}^N} + \beta|\psi_n|^{2\sigma}\psi_n = 0, \tag{1.1}$$

on a N-dimensional lattice which can be finite if supplemented with Dirichlet boundary conditions, or infinite ($n \in \mathbb{Z}^N$). In (1.1), $\epsilon > 0$ is a discretization parameter (usually $\epsilon \sim h^{-2}$ with h being the lattice spacing), and $(\Delta_d\psi)_n$ stands for the N-dimensional discrete Laplacian,

$$(\Delta_d\psi)_{n\in\mathbb{Z}^N} = \sum_{m\in\mathcal{N}_n}\psi_m - 2N\psi_n, \tag{1.2}$$

where $\mathcal{N}_n$ denotes the set of $2N$ nearest neighbors of the point in $\mathbb{Z}^N$ with label n. The nonlinear operator $\mathcal{T}_j$ is defined for every ψ_n, $n = (n_1, n_2, \ldots, n_N) \in \mathbb{Z}^N$, as

$$(\mathcal{T}_j\psi)_{n\in\mathbb{Z}^N} = |\psi_{(n_1,n_2,\ldots,n_j+1,n_{j+1},\ldots,n_N)}|^2 + |\psi_{(n_1,n_2,\ldots,n_j-1,n_{j+1},\ldots,n_N)}|^2,$$
$$j = 1,\ldots,N. \tag{1.3}$$

The nonlinearity parameters $\alpha, \beta \in \mathbb{R}$. In the case $\alpha = 0$, $\beta \neq 0$, one recovers the classical DNLS equation with power nonlinearity. The case where $\alpha, \beta \neq 0$, corresponds to the DNLS equation with nonlinear hopping terms. The DNLS equation (1.1), is a Hamiltonian model with a Hamiltonian of the form

$$\mathcal{H}[\psi] = \epsilon(-\Delta_d \psi, \psi)_2 - \sum_{j=1}^{N} \sum_{n_j=-\infty}^{+\infty} |\psi_{(n_1,n_2,\ldots,n_j,n_{j+1},\ldots,n_N)}|^2 \times |\psi_{(n_1,n_2,\ldots,n_j+1,n_{j+1},\ldots,n_N)}|^2 - \frac{\beta}{\sigma+1} \sum_{n\in\mathbb{Z}^N} |\psi_n|^{2\sigma+2}. \quad (1.4)$$

Let us for convenience discuss the 1D-lattice, where (1.1) reads

$$\mathrm{i}\dot{\psi}_n + \epsilon(\psi_{n-1} - 2\psi_n + \psi_{n+1}) + \alpha\psi_n\left(|\psi_{n+1}|^2 + |\psi_{n-1}|^2\right) + \beta|\psi_n|^{2\sigma}\psi_n = 0, \quad (1.5)$$

with the Hamiltonian

$$\mathcal{H}[\psi] = \epsilon \sum_{n\in\mathbb{Z}} |\psi_{n+1} - \psi_n|^2 - \alpha \sum_{n\in\mathbb{Z}} |\psi_n|^2|\psi_{n+1}|^2 - \frac{\beta}{\sigma+1} \sum_{n\in\mathbb{Z}} |\psi_n|^{2\sigma+2}. \quad (1.6)$$

The Hamiltonian (1.4) and the power (or norm)

$$\mathcal{P}[\psi] = \sum_{n\in\mathbb{Z}^N} |\psi_n|^2 \quad (1.7)$$

are the conserved quantities of this lattice dynamical system.

We will present theoretical and numerical results related to the existence of time-periodic (standing wave) solutions of the form

$$\psi_n(t) = e^{\mathrm{i}\Omega t}\phi_n, \quad \Omega \in \mathbb{R}. \quad (1.8)$$

The physical interest in this particular model stems from various contexts, as the modeling of quantum lattices and waveguide arrays and the approximation of the dynamics of Klein–Gordon (KG) and Fermi–Pasta–Ulam (FPU) chains (Falvo et al. 2006; Claude et al. 1993; Öster et al. 2003, 2004; Öster and Johansson 2005; Johansson 2006). Equation (1.5) for cubic ($\sigma = 1$) nonlinearity corresponds to the classical limit of the quantum DNLS equation introduced in Falvo et al. (2006). In the quantum lattice introduced therein, the inclusion of the nonlinear hopping term allows a fast energy propagation as long as α is high enough with respect to β. Such terms (the additional ones to the classical DNLS with cubic onsite nonlinearity and linear coupling between sites) have appeared in physical considerations within the modeling of waveguide arrays (Öster et al. 2003; Öster and Johansson 2005), establishing that in the case of large penetration length or closely spaced waveguides these terms are not negligible; however, it should be noted that in this case additional terms of the same (cubic) order should be included in the relevant modeling (Öster et al. 2003; Öster and Johansson 2005). Nonlinear hopping terms appear also from FPU and KG chains of anharmonic oscillators coupled with anharmonic inter-site potentials, or mixed FPU/KG chains. The generalized DNLS system of Claude et al. (1993) involving, among others, the nonlinear hopping terms considered therein has been derived as a perturbation of the integrable Ablowitz–Ladik system, by the rotating wave approximation on the FPU chain. A similar DNLS system has been derived in Johansson (2006), approximating the slow dynamics of the fundamental harmonic in the Fourier series expansion of discrete small amplitude modulational waves. The potential relevance of such DNLS systems as models for the energy transport in helical proteins

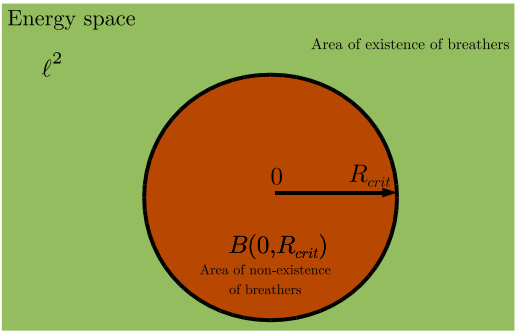

Fig. 1 Simple geometric interpretation of the energy lower bounds obtained by the fixed-point argument: Breathers do not exist in the *darker* (*red*) *area*, the closed ball $B(0, R_{\text{crit}})$ of ℓ^2, centered at 0 and of radius R_{crit}. The *lighter* (*green*) *area* represents the area of the energy space where breather solutions exist. Although the non-existence result does not depend on the dimension and the lattice parameters, the radius R_{crit} of the closed ball $B(0, R_{\text{crit}})$ of non-existence, quantitatively is a function of the lattice parameters α, β, σ, the frequency Ω and the dimension of the lattice N. Note that R_{crit} is not sharp with respect to non-existence. This is suggested from the case for which the excitation threshold R_{thresh} is present. In this case it is possible that $R_{\text{thresh}} > R_{\text{crit}}$, and the *dark* (*red*) *area* is enlarged (Color figure online)

has been discussed in Kundu (2000). However, it is worth remarking that additional terms should also be taken into account therein, as well. Furthermore, such terms have been studied in their own right mathematically while considering the properties of potential traveling waves within a generalized class of DNLS models in Pelinovsky (2006).

In this work, our main scope is to derive lower bounds for the energy of discrete breathers for the DNLS system (1.1) and discuss their relevance as thresholds for their existence. In this point of view, (1.1) seems to be of particular interest due to the interplay and the expected competition of the nonlinear hopping and the generalized power nonlinearities. Extending the arguments based on variational methods (Cuevas et al. 2008a, 2008b, 2010) and the fixed-point approach of Karachalios (2006) to establish the existence of solutions (1.8), we show the existence of lower bounds on the power of breathers on either finite or infinite lattices. The bounds depend explicitly on the dimension, and the nonlinear lattice parameters, as well as on the frequency of the solution. They have a simple geometric interpretation visualized in Fig. 1, elucidated in particular by the fixed-point approach: The energy bounds can be interpreted as the radius R_{crit} of the closed ball centered at 0 in the energy space ℓ^2, denoted by $B(0, R_{\text{crit}})$. Breathers do not exist in the closed ball $B(0, R_{\text{crit}})$, and a non-trivial (e.g. non-zero) breather solution being in $\ell^2 \setminus B(0, R_{\text{crit}})$ should have energy $\mathcal{P} > R_{\text{crit}}^2$. The result is of physical significance related to energy thresholds (where by "energy" here we mean power, or squared ℓ^2 norm) for the formation of breather solutions. In particular, it indicates that for a given set of parameters, no periodic localized solution can have a power less than the prescribed estimates.

It should be remarked that this result is of different nature if compared with the excitation threshold phenomenon of Flach et al. (1997), Weinstein (1999) for discrete breather families, possessing a positive lower bound on their energy when the lattice dimension N is greater than or equal to some critical dimension. In the context

of DNLS systems with power nonlinearity, the restriction for the appearance of the excitation threshold is interpreted in terms of the nonlinearity exponent as $\sigma \geq \frac{2}{N}$ (Weinstein 1999). In this point of view, σ can be considered as critical when $\sigma = \frac{2}{N}$ and supercritical (subcritical) when $\sigma > \frac{2}{N}$ ($\sigma < \frac{2}{N}$), and the excitation threshold exists in the case $\sigma \geq \frac{2}{N}$. It is crucial to remark that the set of parameters for which the excitation threshold $\mathcal{R}_{\text{thresh}}$ is apparent suggests that the energy bounds R_{crit} are not sharp as thresholds for existence/non-existence. In particular, when R_{crit} is the value derived by the fixed-point approach, it is observed that $R_{\text{thresh}} > R_{\text{crit}}$ (Cuevas et al. 2008a, 2010). For further discussions on the excitation threshold for FPU and Klein–Gordon lattices we refer the interested reader to Kastner (2004).

Section 2 is devoted to the derivation of the estimates by variational and energy methods employed in the case of finite lattices, and Sect. 3 is devoted to the fixed-point approach in infinite lattices. While the methods are applicable for both subcritical and supercritical nonlinearities, in the latter case we investigate their interplay with the optimal constant of the discrete interpolation inequality of Weinstein (1999) and its analytical estimation proposed in Cuevas et al. (2009) (Sect. 3.2). In Sect. 4 we perform a numerical analysis testing the lower bounds as thresholds for non-existence of breathers with respect to the variation of the lattice parameters, while Sect. 5 briefly summarizes our conclusions. The previous studies proved the validity of these bounds as energy thresholds for the existence of breather solutions and justified that there are elements of breather families (parametrized by the lattice parameters) which tend to saturate the theoretical bounds in the case of large and small nonlinearity exponents. Aiming to improve this prediction for extended parameter regimes, we consider a refinement of the lower bounds, on account of the finite localization length of the true breather solutions and the expectation that the main contribution to the power comes from the central and adjacent sites, being the most excited. To incorporate this claim in the numerical simulations, we perform a cut-off procedure which considers the part of the system for the oscillators occupying a unit length around the central site plus the adjacent to this unit length as well. This cut-off improves the capture of the contribution of the linear part of the system to the power, manifested in the bounds by the first eigenvalue of the linear operator. The first eigenvalue estimates the contribution of the linear part from below. Contrary to the estimation of the linear part in the real length, its unit length approximation is not negligible since the linear mode over the latter is strongly localized. This is reflected in the numerical simulations performed for the case of the cubic nonlinearity. These calculations reveal that in the weak coupling regime the bounds are getting closer to the numerical power, and in some cases provide its accurate prediction. This quantitative response is observed in particular versus the nonlinear hopping parameter α. The accuracy of the estimates indicates that the approach presented can be promising in a study of DNLS systems encountered in the aforementioned applications, involving the full expansion of nonlinear hopping terms being, however, of the same order.

We conclude the introductory section, by mentioning that although our results concern both the cases of finite and infinite lattices the term "breather" has been used for the standing wave solutions (1.8) in the finite case, only for the sake of brevity. The important issue of the localization properties of the solutions in the transition from finite to infinite lattice is not addressed in the present work. We refer to Penati and

Paleari (2012) for a detailed discussion of the spatial decay and stability properties of the solutions when the lattice size is varied for small-amplitudes (i.e., near the continuum limit), as well as, for relative localization estimates. For the convergence of solutions, defined by constrained variational problems in finite lattices to unimodal and even profile breather solutions (centered on a site or between two lattice sites) in infinite lattices, we refer the interested reader to Herrmann (2011).

Preliminaries For convenience, we recall from Cuevas et al. (2008a, 2008b) some preliminary information on various norms and quantities, which will be thoroughly used in what follows.

The finite-dimensional problem is formulated in the finite-dimensional subspaces of the sequence spaces ℓ^p, $1 \le p \le \infty$,

$$\ell^p\big(\mathbb{Z}_K^N\big) = \big\{\phi \in \ell^p : \phi_n = 0 \text{ for } |||n||| > K\big\}, \tag{1.9}$$

where $|||n||| = \max_{1\le i\le N} |n_i|$ for $n = (n_1, n_2, \ldots, n_N) \in \mathbb{Z}^N$. Note that in the case of the infinite lattice $\mathbb{Z}^N$

$$\|\phi\|_q \le \|\phi\|_p, \quad 1 \le p \le q \le \infty \tag{1.10}$$

$$0 \le \epsilon(-\Delta_d\phi, \phi)_2 \le 4\epsilon N \sum_{n\in\mathbb{Z}^N} |\phi_n|^2. \tag{1.11}$$

For the finite-dimensional case we find that $\ell^p(\mathbb{Z}_K^N) \equiv \mathbb{C}^{(2K+1)^N}$, endowed with the norm

$$\|\phi\|_p = \Bigg(\sum_{|||n|||\le K} |\phi_n|^p\Bigg)^{\frac{1}{p}},$$

and that the well known equivalence of norms,

$$\|\phi\|_q \le \|\phi\|_p \le (2K+1)^{\frac{N(q-p)}{qp}} \|\phi\|_q, \quad 1 \le p \le q < \infty, \tag{1.12}$$

holds.

At this point let us remark on some basic facts on the eigenvalues of the discrete Dirichlet Laplacian, since they will naturally appear in the estimates that will be derived and have an important role in the numerical simulations. For the 1D-lattice of $K+2$ oscillators, $n = 0, \ldots, K+1$, let us consider the discrete eigenvalue problem for $\phi_n \in \mathbb{R}$,

$$-\epsilon\Delta_d\phi_n = \mu\phi_n, \quad n = 1, \ldots K, \tag{1.13}$$

with Dirichlet boundary conditions, $\phi_0 = \phi_{K+1} = 0$. Starting from the standard case

$$\epsilon = \frac{1}{h^2} \quad \text{where } h = \frac{L}{K+1}, \tag{1.14}$$

where L denotes the length of the chain, the eigenvalues are

$$\mu_n(h) = \frac{4}{h^2}\sin^2\left(\frac{n\pi h}{2L}\right) = \frac{4(K+1)^2}{L^2}\sin^2\left(\frac{n\pi}{2(K+1)}\right), \quad n = 1, \ldots, K.$$

Thus, in the case (1.14) the principal eigenvalue is

$$\mu_1(h) = \frac{4}{h^2}\sin^2\left(\frac{\pi h}{2L}\right) = \frac{4(K+1)^2}{L^2}\sin^2\left(\frac{\pi}{2(K+1)}\right). \tag{1.15}$$

The discrete system is modeled when $h = O(1)$, and in the limits $h \to 0$ and $h \to \infty$ we have

$$\lim_{h\to 0}\mu_1(h) = \lambda_1 = \frac{\pi^2}{L^2} \quad \text{(continuous limit)}, \tag{1.16}$$

$$\lim_{h\to\infty}\mu_1(h) = 0 \quad \text{(anticontinuous limit)}. \tag{1.17}$$

In the particular case of $L = 1$ we have

$$\lim_{h\to 0}\mu_1(h) = \lambda_1 = \pi^2, \tag{1.18}$$

$$4 \le \mu_1(h) \le \pi^2, \quad \text{for } 0 < h \le 1. \tag{1.19}$$

In a general discrete case the parameter $\epsilon > 0$ can be either related or not related with the lattice spacing h. As an example for the latter, we may fix the linear coupling constant $\epsilon > 0$, varying the number of oscillators, equidistanced with lattice spacing $h = \frac{L}{K+1}$. We have

$$\begin{aligned} &\mu_1(h) = 4\epsilon\sin^2\left(\frac{\pi h}{2L}\right) = 4\epsilon\sin^2\left(\frac{\pi}{2(K+1)}\right), \\ &\lim_{h\to 0}\mu_1(h) = 0 \quad (h \to 0 \text{ when } K \to \infty), \end{aligned} \tag{1.20}$$

$$0 \le \mu_1(h) \le 4\epsilon. \tag{1.21}$$

Increasing K, (1.20)–(1.21) can be considered as a particular approximation *of an infinite lattice*. Note that in the case of the infinite lattice $\mathbb{Z}^N$, for the discrete Laplacian with $\epsilon = 1$, we have $\sigma(-\Delta_d) \subseteq [0, 4N]$.

Relations (1.15) and (1.16), (1.17) are valid for a general coupling (depending or not depending on the lattice spacing) behaving as $\epsilon \sim \frac{1}{h^2}$ with ϵ sufficiently large. Similar observations are valid in the case of the N-dimensional discrete Laplacian.

Finally, we recall the variational characterization of the eigenvalues of the discrete Laplacian in the finite-dimensional subspaces $\ell^2(\mathbb{Z}_K^N)$, showing that $\mu_1 > 0$, can be characterized as

$$\mu_1 = \inf_{\substack{\phi\in\ell^2(\mathbb{Z}_K^N)\\ \phi\neq 0}} \frac{(-\epsilon\Delta_d\phi,\phi)_2}{\sum_{|||n|||\le K}|\phi_n|^2}. \tag{1.22}$$

Then, (1.22) implies the inequality

$$\mu_1 \sum_{|||n|||\le K}|\phi_n|^2 \le \epsilon(-\Delta_d\phi,\phi)_2 \le 4\epsilon N \sum_{|||n|||\le K}|\phi_n|^2. \tag{1.23}$$

2 Finite Dimensional Lattices

This section is devoted to the DNLS equation with nonlinear hopping terms $\alpha, \beta \neq 0$, supplemented with Dirichlet boundary conditions

$$\mathrm{i}\dot{\psi}_n + \epsilon(\Delta_d \psi)_n + \alpha\psi_n \sum_{j=1}^{N} (\mathcal{T}_j \psi)_{n\in\mathbb{Z}^N} + \beta|\psi_n|^{2\sigma}\psi_n = 0, \tag{2.1}$$

$$\psi_n = 0, \quad \|n\| > K. \tag{2.2}$$

We will employ a constrained variational approach on the nonlinear energy functional involving the nonlinear hopping term. Noticing that the existence result can be established by minimization of the Hamiltonian or by application of min-max methods (e.g. mountain pass type theorems), the usage of alternative functionals may reveal interesting conditions on the nonlinearity parameters. An example is given in Cuevas et al. (2010, Sects. 2.2 and 2.3, pp. 9–18), where the minimization of a linear energy functional under a nonlinear constraint verified conditions for the co-existence of breather profiles. For instance, this alternative approach for (2.1) will show the existence of a regime for the hopping parameter α where an upper bound for the power is valid (see Remark 2.4).

Note that the case of Dirichlet boundary conditions is of interest, in particular for numerical simulations; since the infinite lattice cannot be modeled numerically, numerical investigations should consider finite lattices with Dirichlet or periodic boundary conditions. The latter should be imposed for moving breathers when reaching the boundary. We expect that the variational approach can be applied in the case of periodic boundary conditions, but the details have to be checked.

We shall consider first the focusing case for the parameters $\alpha, \beta > 0$ and we shall briefly comment on the defocusing one $\alpha, \beta < 0$ which can be treated similarly.

2.1 The Focusing Case $\alpha, \beta > 0$—Solutions $\psi_n(t) = e^{\mathrm{i}\Omega t}\phi_n$, $\Omega > 0$

Substitution of the solution (1.8) into (1.1) shows that ϕ_n satisfies the system of algebraic equations

$$-\epsilon(\Delta_d \phi)_n + \Omega\phi_n - \alpha\phi_n \sum_{j=1}^{N} (\mathcal{T}_j \phi)_{n\in\mathbb{Z}^N} - \beta|\phi_n|^{2\sigma}\phi_n = 0, \quad \Omega \in \mathbb{R}, \|n\| \leq K, \tag{2.3}$$

$$\phi_n = 0, \quad \|n\| > K. \tag{2.4}$$

Let us note that in the anticontinuous limit $\epsilon = 0$, the corresponding energy equation reads

$$\Omega \sum_{\|n\|\leq K} |\phi_n|^2 = \alpha \sum_{\|n\|\leq K} |\phi_n|^2 \sum_{j=1}^{N} (\mathcal{T}_j \phi)_{n\in\mathbb{Z}^N} + \beta \sum_{\|n\|\leq K} |\phi_n|^{2\sigma+2}, \quad \alpha, \beta > 0.$$

Its positive right-hand side, implies directly that in the limit $\epsilon = 0$, the focusing case supports only solutions with $\Omega > 0$.

For $\epsilon > 0$ we will also restrict our considerations to the case of solutions with $\Omega > 0$. We recall two auxiliary lemmas regarding the differentiability of the nonlinear terms if viewed as nonlinear functionals, which can be proved as in Karachalios (2006, Lemma 2.3, p. 121).

Lemma 2.1 *Let $\phi \in \ell^2$. Then the functional*

$$\mathcal{V}(\phi) = \sum_{j=1}^{N} \sum_{n_j=-\infty}^{+\infty} |\phi_{(n_1,n_2,\ldots,n_j,n_{j+1},\ldots,n_N)}|^2 |\phi_{(n_1,n_2,\ldots,n_j+1,n_{j+1},\ldots,n_N)}|^2,$$

is a $\mathrm{C}^1(\ell^2,\mathbb{R})$ functional and for all $\psi \in \ell^2$,

$$\begin{aligned}\left\langle \mathcal{V}'(\phi), \psi \right\rangle = {} & 2\mathrm{Re} \sum_{j=1}^{N} \sum_{n_j=-\infty}^{+\infty} |\phi_{(n_1,n_2,\ldots,n_j+1,n_{j+1},\ldots,n_N)}|^2 \\ & \times \phi_{(n_1,n_2,\ldots,n_j,n_{j+1},\ldots,n_N)} \overline{\psi}_{(n_1,n_2,\ldots,n_j,n_{j+1},\ldots,n_N)} \\ & + 2\mathrm{Re} \sum_{j=1}^{N} \sum_{n_j=-\infty}^{+\infty} |\phi_{(n_1,n_2,\ldots,n_j-1,n_{j+1},\ldots,n_N)}|^2 \\ & \times \phi_{(n_1,n_2,\ldots,n_j,n_{j+1},\ldots,n_N)} \overline{\psi}_{(n_1,n_2,\ldots,n_j,n_{j+1},\ldots,n_N)}. \end{aligned} \tag{2.5}$$

Lemma 2.2 *Let $\phi \in \ell^2$. Then the functional*

$$\mathcal{L}(\phi) = \sum_{n \in \mathbb{Z}^N} |\phi_n|^{2\sigma+2}$$

is a $\mathrm{C}^1(\ell^2,\mathbb{R})$ functional and

$$\left\langle \mathcal{L}'(\phi), \psi \right\rangle = 2(\sigma+1)\mathrm{Re} \sum_{n \in \mathbb{Z}^N} |\phi_n|^{2\sigma} \phi_n \overline{\psi}_n. \tag{2.6}$$

The two Lemmas 2.1 and 2.2 remain valid in the case of the finite lattice (space $\ell^2(\mathbb{Z}_K^N)$).

The first result on the existence of time-periodic solutions (1.8) of (2.1), is via a constrained minimization problem for the functional

$$\mathcal{E}[\phi] := \epsilon(-\Delta_d \phi, \phi)_2 + \Omega \sum_{n \in \mathbb{Z}^N} |\phi_n|^2 - \alpha \mathcal{V}(\phi), \quad \Omega > 0, \alpha > 0. \tag{2.7}$$

Theorem 2.3

A. *Consider the variational problem on $\ell^2(\mathbb{Z}_K^N)$*

$$\inf\left\{ \mathcal{E}[\phi] : \frac{1}{\sigma+1}\mathcal{L}[\phi] = M \right\}, \tag{2.8}$$

for some $\Omega > 0$. Then, there exists a minimizer $\hat{\phi} \in \ell^2(\mathbb{Z}_K^N)$ for the variational problem (2.8) and $\beta(M) > 0$, both satisfying the Euler–Lagrange equation (2.3)–(2.4) and $\sum_{n \in \mathbb{Z}_K^N} |\hat{\phi}_n|^{2\sigma+2} = M(\sigma+1)$.

B. *Assume that the power of a solution of the problem* (2.3)–(2.4) *is* $\mathcal{P}[\hat{\phi}] = R^2$. *Then the power satisfies the lower bound*

$$R_{*,f}^2 < R^2 = \mathcal{P}[\hat{\phi}], \tag{2.9}$$

where $R_{*,f}$ *denotes the unique positive root of the algebraic equation*

$$\beta\chi^{2\sigma} + 2\alpha N\chi^2 - (\mu_1 + \Omega) = 0. \tag{2.10}$$

C. *We assume that*

$$\sigma > 1. \tag{2.11}$$

Then a breather solution of (1.1) *satisfies the lower bound*

$$\left[\frac{1}{2\beta}\left(\Omega + \mu_1 - \frac{(2\alpha N)^{\frac{\sigma}{\sigma-1}}}{(\beta\sigma)^{\frac{1}{\sigma-1}}}\frac{\sigma-1}{\sigma}\right)\right]^{\frac{1}{\sigma}} < R^2, \tag{2.12}$$

in either one of the cases:

(i) (*lattice spacing condition*) *For all* $\Omega > 0$ *if*

$$\epsilon > \frac{(2\alpha N)^{\frac{\sigma}{\sigma-1}}}{(\beta\sigma)^{\frac{1}{\sigma-1}}}\frac{\sigma-1}{\lambda_1\sigma}. \tag{2.13}$$

(ii) (*frequency condition*) *For all* $\epsilon > 0$ *if*

$$\Omega > \frac{(2\alpha N)^{\frac{\sigma}{\sigma-1}}}{(\beta\sigma)^{\frac{1}{\sigma-1}}}\frac{\sigma-1}{\sigma}. \tag{2.14}$$

Proof A. We consider the set

$$B_\sigma = \left\{\phi \in \ell^2\big(\mathbb{Z}_K^N\big) : \frac{1}{\sigma+1}\mathcal{L}[\phi] = M\right\}.$$

From Lemma 2.5, we may easily infer that $\mathcal{E} : B_\sigma \to \mathbb{R}$ is a C^1-functional. Moreover, by using inequality (1.12), we deduce that

$$\begin{aligned}
\mathcal{E}[\phi] &\geq -\alpha\mathcal{V}[\phi] \\
&\geq -\alpha N \sum_{n\in\mathbb{Z}^N} |\phi_n|^2\|\phi\|_2^2 \geq -\alpha N\|\phi\|_2^4 \\
&\geq -\alpha N(2K+1)^{\frac{2N\sigma}{\sigma+1}}\big(\mathcal{L}[\phi]\big)^{\frac{2}{\sigma+1}} \\
&= -\alpha N(2K+1)^{\frac{2N\sigma}{\sigma+1}}\big(M(\sigma+1)\big)^{\frac{2}{\sigma+1}}.
\end{aligned}$$

Therefore, the functional $\mathcal{E} : B_\sigma \to \mathbb{R}$ is bounded from below. By the definition of the set B_σ and the fact that we are restricted to the finite-dimensional space $\ell^2(\mathbb{Z}_K^N)$, it immediately follows that any minimizing sequence associated with the variational problem (2.8) is precompact. Hence, by the Weierstraß minimization theorem (Zeidler 1995, Proposition 8, p. 37), any minimizing sequence has a subsequence converging to a minimizer and $\mathcal{E}$ attains its infimum at a point $\hat{\phi}$ in B_σ. To derive the variational equation (2.3), we consider first the C^1-functional (due to Lemma 2.2)

$$\mathcal{L}_M[\phi] = \frac{1}{\sigma+1}\mathcal{L}[\phi] - M,$$

and we observe that for any $\phi \in B_\sigma$

$$\big\langle \mathcal{L}'_M[\phi], \phi \big\rangle = 2\mathcal{L}[\phi] = 2M.$$

Thus, the Regular Value Theorem (Chow and Hale 1982, Sect. 2.9; Haskins and Speight 2002, Appendix A, p. 556) implies that the set $B_\sigma = \mathcal{L}_M^{-1}(0)$ is a C^1-submanifold of $\ell^2(\mathbb{Z}_K^N)$. Application of the Lagrange multiplier rule implies the existence of a parameter $\beta = \beta(M) \in \mathbb{R}$, such that

$$\begin{aligned}\big\langle \mathcal{E}'[\hat\phi] - \beta\mathcal{L}'_M[\hat\phi], \psi\big\rangle &= 2\epsilon(-\Delta_d\hat\phi, \psi)_2 + 2\Omega\mathrm{Re}\sum_{n\in\mathbb{Z}^N}\hat\phi_n\overline{\psi}_n \\ &\quad - 2\alpha\mathrm{Re}\sum_{j=1}^{N}\sum_{n_j=-\infty}^{+\infty}|\hat\phi_{(n_1,n_2,\ldots,n_j+1,n_{j+1},\ldots,n_N)}|^2 \\ &\quad \times \hat\phi_{(n_1,n_2,\ldots,n_j,n_{j+1},\ldots,n_N)}\overline{\psi}_{(n_1,n_2,\ldots,n_j,n_{j+1},\ldots,n_N)} \\ &\quad - 2\alpha\mathrm{Re}\sum_{j=1}^{N}\sum_{n_j=-\infty}^{+\infty}|\hat\phi_{(n_1,n_2,\ldots,n_j-1,n_{j+1},\ldots,n_N)}|^2 \\ &\quad \times \hat\phi_{(n_1,n_2,\ldots,n_j,n_{j+1},\ldots,n_N)}\overline{\psi}_{(n_1,n_2,\ldots,n_j,n_{j+1},\ldots,n_N)} \\ &\quad - 2\beta\mathrm{Re}\sum_{n\in\mathbb{Z}^N}|\hat\phi_n|^{2\sigma}\hat\phi_n\overline{\psi}_n = 0, \quad \text{for all } \psi \in \ell^2\big(\mathbb{Z}_K^N\big).\end{aligned} \tag{2.15}$$

Setting $\psi = \hat\phi$ in (2.15), we find that

$$\begin{aligned}\mathcal{F}[\hat\phi] &:= \epsilon(-\Delta_d\hat\phi, \hat\phi)_2 + \Omega\sum_{n\in\mathbb{Z}^N}|\hat\phi_n|^2 \\ &\quad - 2\alpha\mathrm{Re}\sum_{j=1}^{N}\sum_{n_j=-\infty}^{+\infty}|\hat\phi_{(n_1,n_2,\ldots,n_j+1,n_{j+1},\ldots,n_N)}|^2|\hat\phi_{(n_1,n_2,\ldots,n_j,n_{j+1},\ldots,n_N)}|^2 \\ &\quad - 2\alpha\mathrm{Re}\sum_{j=1}^{N}\sum_{n_j=-\infty}^{+\infty}|\hat\phi_{(n_1,n_2,\ldots,n_j-1,n_{j+1},\ldots,n_N)}|^2|\hat\phi_{(n_1,n_2,\ldots,n_j,n_{j+1},\ldots,n_N)}|^2 \\ &= \beta\sum_{n\in\mathbb{Z}^N}|\hat\phi_n|^{2\sigma+2}.\end{aligned} \tag{2.16}$$

By virtue of (1.23), we deduce that the estimate

$$\begin{aligned}\mathcal{F}[\hat\phi] &\geq \mu_1\|\hat\phi\|_2^2 + \Omega\|\hat\phi\|_2^2 - 2\alpha N\sum_{n\in\mathbb{Z}^N}\|\hat\phi\|_2^2|\hat\phi_n|^2 \\ &\geq \mu_1\|\hat\phi\|_2^2 + \Omega\|\hat\phi\|_2^2 - 2\alpha N\|\hat\phi\|_2^4\end{aligned} \tag{2.17}$$

holds. Let us assume that $\mathcal{P}[\hat\phi] = \|\hat\phi\|_2^2 = R^2$. Then from (2.17), we obtain

$$\mathcal{F}[\hat\phi] \geq R^2\big(\mu_1 + \Omega - 2\alpha N R^2\big).$$

Therefore, assuming that

$$R^2 < \frac{\mu_1 + \Omega}{2\alpha N}, \tag{2.18}$$

or assuming in terms of α that

$$0 < \alpha < \frac{\mu_1 + \Omega}{2NR^2}, \tag{2.19}$$

we deduce that $\mathcal{F}[\hat{\phi}] > 0$. Since $\hat{\phi} \in B_\sigma$ cannot be identically zero and $\mathcal{F}[\hat{\phi}] > 0$, it follows from (2.16) that $\beta > 0$. Summarizing, we have proved that for given $\Omega > 0$, there exists a minimizer $\hat{\phi}$ and a Lagrange multiplier $\beta > 0$ solving the variational equation (2.15). Clearly a solution of the variational equation (2.15) is a solution of the Euler–Lagrange equation (2.3)–(2.4).

B. It is necessary to verify first that any solution $\hat{\phi}$ of (2.3)–(2.4) is a solution of the minimization problem (2.8). Indeed, if $\hat{\phi}$ is a solution of (2.3)–(2.4), multiplying (2.3) by $\hat{\phi}$ in the $\ell^2(\mathbb{Z}_K^N)$ and using the Dirichlet boundary conditions we infer that $\hat{\phi}$ satisfies (2.16), written as

$$\mathcal{F}[\hat{\phi}] = \beta \mathcal{L}[\hat{\phi}]. \tag{2.20}$$

Then, due to Lemmas 2.1 and 2.2, $\hat{\phi}$ solves also the equation

$$\big\langle \mathcal{F}'[\hat{\phi}], \psi \big\rangle = \beta \big\langle \mathcal{L}'[\hat{\phi}], \psi \big\rangle, \quad \text{for all } \psi \in \ell^2\big(\mathbb{Z}_K^N\big).$$

Comparing (2.15) with (2.16) it can be easily seen that the equation above is equivalent to

$$\big\langle \mathcal{E}'[\hat{\phi}], \psi \big\rangle = \beta \big\langle \mathcal{L}'[\hat{\phi}], \psi \big\rangle, \quad \text{for all } \psi \in \ell^2\big(\mathbb{Z}_K^N\big), \tag{2.21}$$

thus, $\hat{\phi}$ is a minimizer of the minimization problem (2.8). The converse follows immediately by (2.21) and the fact that in the discrete setting a "weak solution" of (2.21) coincides with a solution of (2.3)–(2.4). Furthermore, by setting $\psi = \hat{\phi}$ in (2.21) we recover that $\hat{\phi}$ satisfies (2.20).

Assuming now that the power of the solution of (2.3) is $\mathcal{P}[\hat{\phi}] = \|\hat{\phi}\|_2^2 = R^2$, by using (1.12) and (1.23) we find from (2.20) that R satisfies the inequality

$$\mu_1 + \Omega \le 2\alpha N R^2 + \beta R^{2\sigma}. \tag{2.22}$$

The algebraic equation (2.10) considered for $\chi \in [0, \infty)$, has exactly one positive root $0 < R_{*,f}$. Then, comparison of (2.10) with inequality (2.22), implies that the power $\mathcal{P}[\hat{\phi}]$ must satisfy the lower bound (2.9).

C. Applying Young's inequality

$$ab < \frac{\hat{\epsilon}}{p} a^p + \frac{1}{q\hat{\epsilon}^{q/p}} b^q, \quad a, b > 0 \text{ for any } \hat{\epsilon} > 0, 1/p + 1/q = 1,$$

with $p = \sigma$, $q = \frac{\sigma}{\sigma - 1}$ $a = R^2$, $b = 2\alpha N$ and $\hat{\epsilon} = \beta\sigma$ we get

$$2\alpha R^2 \le \beta R^{2\sigma} + \frac{(2\alpha N)^{\frac{\sigma}{\sigma-1}}}{(\beta\sigma)^{\frac{1}{\sigma-1}}} \frac{\sigma - 1}{\sigma}. \tag{2.23}$$

Inserting (2.23) into (2.22) we derive the lower bound (2.12). □

Remark 2.4

1. (The lower bound for the cubic nonlinearity.) For the case of cubic nonlinearity $\sigma = 1$, inequality (2.22) implies that the power of the periodic solution $\psi_n(t) = e^{i\Omega t}\hat{\phi}_n$, $\Omega > 0$ must satisfy the lower bound

$$\frac{\mu_1 + \Omega}{2\alpha N + \beta} < R^2 = \mathcal{P}[\hat{\phi}]. \tag{2.24}$$

2. (Interpretation of condition (2.18).) The result of Theorem 2.3 establishes for arbitrary given $\Omega > 0$ and $\alpha > 0$, the existence of a non-trivial $\hat{\phi} \in \ell^2(\mathbb{Z}_K^N)$ and the existence of $\beta > 0$ as a Lagrange multiplier such that $\psi_n(t) = e^{i\Omega t}\hat{\phi}_n$, solves (2.1) with $\beta > 0$ as a parameter for the power nonlinearity. On the account of this result, the meaning of condition (2.18) is *that there exists* $\beta > 0$ *and a range of the hopping parameter* $0 < \alpha < \alpha^*$ *for which the associated minimizer* $\hat{\phi}$ *has power satisfying the upper bound*

$$\mathcal{P}[\hat{\phi}] = R^2 < \frac{\mu_1 + \Omega}{2\alpha N}. \tag{2.25}$$

   Note that the existence of the range of the hopping parameter α stated above is also established by (2.18)—see (2.19).
3. (Case $\alpha \to 0$, $\beta > 0$-DNLS with power nonlinearity.) The proof of Theorem 2.3 remains valid for the case $\alpha = 0$, where one has to consider the constrained minimization problem (2.8) for the functional $\mathcal{E}$, setting $\alpha = 0$. Thus for the classical DNLS with power nonlinearity we recover from inequality (2.22), the lower bound

$$\left[\frac{\mu_1 + \Omega}{\beta}\right]^{\frac{1}{\sigma}} < R^2 = \mathcal{P}[\hat{\phi}]. \tag{2.26}$$

   The lower bound (2.26) is the same as (5.27) and (5.31) of Cuevas et al. (2008a) for the DNLS with power nonlinearity.

2.2 The Defocusing Case $\alpha, \beta < 0$—Solutions $\psi_n(t) = e^{-\mathrm{i}\Omega t}\phi_n$, $\Omega > 0$

We shall briefly comment on the existence of breather solutions, for the case of negative nonlinear parameters $\alpha, \beta < 0$. We set for convenience $\alpha = -\kappa$, $\beta = -\lambda$ where $\kappa, \lambda > 0$. It should be remarked that the case of negative parameters can be reduced to the case of positive ones, under the staggering transformation. We recall that this transformation is defined as

$$\psi_n \to (-1)^{|n|}\psi_n, \quad |n| = \sum_{i=1}^{N} n_i, \tag{2.27}$$

(see e.g. the discussion of Kevrekidis et al. 2006, p. 7). The case of negative parameters, corresponds to the existence problem for solutions

$$\psi_n(t) = e^{-\mathrm{i}\Omega t}\phi_n, \quad \Omega > 0, \tag{2.28}$$

where ϕ_n satisfies the system of algebraic equations

$$-\epsilon(\Delta_d\phi)_n - \Omega\phi_n + \kappa\phi_n \sum_{j=1}^{N} (\mathcal{T}_j\phi)_{n\in\mathbb{Z}^N} + \lambda|\phi_n|^{2\sigma}\phi_n = 0, \Omega > 0, \quad \|n\| \le K, \tag{2.29}$$

$$\phi_n = 0, \quad \|n\| > K. \tag{2.30}$$

The proof of the existence of breather solutions (2.28) is very similar to that of Theorem 2.3, and we refrain from giving the details. We just note that the constrained minimization problem will consider the C^1-functional

$$\mathcal{E}[\phi] := \epsilon(-\Delta_d\phi, \phi)_2 - \Omega \sum_{n\in\mathbb{Z}^N} |\phi_n|^2 + \kappa\mathcal{V}(\phi), \Omega > 0, \quad \kappa > 0. \tag{2.31}$$

Theorem 2.5

A. *Consider the variational problem on* $\ell^2(\mathbb{Z}_K^N)$

$$\inf\left\{\mathcal{E}[\phi] : \frac{1}{\sigma+1}\mathcal{L}[\phi] = M\right\} \tag{2.32}$$

for some $\Omega > 0$. *Assume further that*

$$\Omega > 4\epsilon N. \tag{2.33}$$

Then, there exists a minimizer $\phi^* \in \ell^2(\mathbb{Z}_K^N)$ *for the variational problem* (2.32) *and* $\lambda(M) > 0$, *satisfying both the Euler–Lagrange equation* (2.29)–(2.30) *and* $\sum_{n\in\mathbb{Z}^N} |\phi_n^*|^{2\sigma+2} = M$.

B. *Assume that* (2.33) *holds and that the power of a solution of the problem* (2.29)–(2.30) *is* $\mathcal{P}[\phi^*] = R^2$. *Then the power satisfies the lower bound*

$$R_{*,d}^2 < R^2 = \mathcal{P}[\phi^*], \tag{2.34}$$

where $R_{*,d}$ *denotes the unique positive root of the equation*

$$\lambda\chi^{2\sigma} + 2\kappa N\chi^2 - (\Omega - 4\epsilon N) = 0. \tag{2.35}$$

C. *Let* $\sigma > 1$ *and assume that*

$$\Omega > 4\epsilon N + \frac{\sigma-1}{\lambda^{\frac{1}{\sigma-1}}}\left(\frac{2\kappa N}{\sigma}\right)^{\frac{\sigma}{\sigma-1}}. \tag{2.36}$$

Then the power satisfies the lower bound

$$\left[\frac{1}{2\lambda}\left(\Omega - 4\epsilon N - \frac{(2\kappa N)^{\frac{\sigma}{\sigma-1}}}{(\lambda\sigma)^{\frac{1}{\sigma-1}}}\frac{\sigma-1}{\sigma}\right)\right]^{\frac{1}{\sigma}} < R^2 = \mathcal{P}[\phi^*]. \tag{2.37}$$

Remark 2.6

1. (The lower bound for the cubic nonlinearity.) For the case of negative parameters $\alpha = -\kappa, \beta = -\lambda$, $\kappa, \lambda > 0$ and of cubic nonlinearity $\sigma = 1$, the power of the periodic solution $\psi_n(t) = e^{-i\Omega t}\hat{\phi}_n$, $\Omega > 0$ must satisfy the lower bound

$$\frac{\Omega - 4\epsilon N}{2\kappa N + \lambda} < R^2 = \mathcal{P}[\phi^*], \quad \Omega > 4\epsilon N. \tag{2.38}$$

2. (An upper bound for some range of parameters.) The result of Theorem 2.5 establishes for given $\Omega > 4\epsilon$ and $\alpha = -\kappa < 0$, the existence of a non-trivial $\phi^* \in \ell^2(\mathbb{Z}_K^N)$ and the existence of $\beta = -\lambda < 0$ such that $\psi_n(t) = e^{-i\Omega t}\phi_n^*$, solves equation (2.1) with $\beta > 0$ as a parameter for the power nonlinearity. As in Remark 2.4-2, a similar condition to (2.18) can be derived, implying that there exist a parameter λ and a range for the hopping parameter κ for which the corresponding minimizer ϕ^* has power satisfying the upper bound

$$\mathcal{P}\big[\phi^*\big] < \frac{\Omega - 4\epsilon N}{2\kappa N}, \quad \Omega > 4\epsilon N. \tag{2.39}$$

3. (Case $\kappa \to 0, \lambda > 0$-DNLS with *defocusing* power nonlinearity.) The proof of Theorem 2.5 remains valid for the case $\kappa = 0$, where one has to consider the constrained minimization problem (2.32) for the functional $\mathcal{E}$, setting $\kappa = 0$. Thus for the classical DNLS with power nonlinearity we recover the lower bound

$$\left[\frac{\Omega - 4\epsilon N}{\lambda}\right]^{\frac{1}{\sigma}} < R^2 = \mathcal{P}\big[\phi^*\big], \quad \Omega > 4\epsilon N. \tag{2.40}$$

The lower bound (2.26) is exactly the same as that derived in Cuevas et al. (2008a) for the one-dimensional DNLS with defocusing power nonlinearity.

4. Condition (2.33) is related with the extension of the phonon band for defocusing-type DNLS equations, to the interval $[0, 4\epsilon N]$. Combining the results of Theorem 2.3 for the focusing case and of Theorem 2.5 for the defocusing one, we see that for breathers in the ansatz $\psi_n = e^{-\mathrm{i}\Omega t}\phi_n$, frequencies $\Omega \in \mathbb{R}$, must lie in the intervals $\Omega > 4\epsilon N$ (defocusing case) and $\Omega < 0$ (focusing case).

3 Infinite $\mathbb{Z}^N$, $N \geq 1$ Lattices

For the infinite lattice $\mathbb{Z}^N$, we will consider the problem of energy bounds for breathers of the DNLS (1.1) by a fixed-point method. The method establishes that the stationary problem (2.3) defines a locally Lipschitz map on the phase space ℓ^2. When the map is a contraction, gives rise only to the trivial solution. The Lipschitz constant for the contraction mapping defines the critical power above which we should expect existence of breathers. Below this critical power there is non-existence of breather solutions. The Lipschitz constant contains all the lattice parameters, including the dimension of the lattice and the frequency of the solution.

3.1 The Case $\alpha, \beta > 0$—Solutions $\psi_n(t) = e^{\mathrm{i}\Omega t}$, $\Omega > 0$: Fixed-Point Method

The infinite system of algebraic equations (2.3) for breathers in the case of the infinite lattice will be treated by a fixed-point argument. We recall that the linear and continuous operator

$$-\epsilon\Delta_d + \Omega: \quad \ell^2 \to \ell^2, \tag{3.1}$$

satisfies the assumptions of Lax–Milgram Theorem (Zeidler 1990, Theorem 18.E, p. 68), since

$$\epsilon(-\Delta_d\phi,\phi)_2+\Omega\|\phi\|_2^2\geq\Omega\|\phi\|_2^2\quad\text{for all }\phi\in\ell^2.$$

This is the first step to verify that for given $z\in\ell^2$, the *auxiliary problem* defined by the linear operator equation

$$-\epsilon\Delta_d\phi_n+\Omega\phi_n=\alpha z_n\sum_{j=1}^{N}(\mathcal{T}_j z)_{n\in\mathbb{Z}^N}+\beta|z_n|^{2\sigma}z_n,\tag{3.2}$$

has a unique solution $\phi\in\ell^2$. The second step, according the Lax–Milgram Theorem, is to justify that the right-hand side of (3.2) is in ℓ^2 if $z\in\ell^2$. Indeed, by using the inequality

$$\sum_{n\in\mathbb{Z}^N}|\phi_n|^p\leq\Bigg(\sum_{n\in\mathbb{Z}^N}|\phi_n|^q\Bigg)^{\frac{p}{q}},\quad\text{for all }1\leq q\leq p\leq\infty,\tag{3.3}$$

for $p=4\sigma+2$ and $q=2$, it follows that

$$\big\||z|^{2\sigma}z\big\|_2^2\leq\sum_{n\in\mathbb{Z}^N}|z_n|^{4\sigma+2}\leq\|z\|_2^{4\sigma+2}.\tag{3.4}$$

Furthermore, for the nonlinear map $\mathcal{J}:\ell^2\to\ell^2$,

$$\mathcal{J}[z_n]=z_n\sum_{j=1}^{N}(\mathcal{T}_j z)_{n\in\mathbb{Z}^N},$$

we have

$$\big\|\mathcal{J}[z]\big\|_2^2\leq 2N\sup_{n\in\mathbb{Z}^N}|z_n|^2\sum_{n\in\mathbb{Z}^N}|z_n|^2\leq 2N\|z\|_2^4.$$

Therefore we are allowed to define the map $\mathcal{A}:\ell^2\to\ell^2$, by $\mathcal{A}(z):=\phi$, where ϕ is a unique solution of the operator equation (3.2). Clearly the map $\mathcal{A}$ is well defined. Let ζ,ξ be in the closed ball

$$B_R:=\big\{z\in\ell^2:\|z\|_{\ell^2}\leq R\big\},$$

and $\phi=\mathcal{A}(\zeta)$, $\psi=\mathcal{A}(\xi)$. The difference $\chi:=\phi-\psi$ satisfies the equation

$$-\epsilon\Delta_d\chi_n+\Omega\chi_n=\alpha\big(\mathcal{J}[\zeta_n]-\mathcal{J}[\xi_n]\big)+\beta\big(|\zeta_n|^{2\sigma}\zeta_n-|\xi_n|^{2\sigma}\xi_n\big).\tag{3.5}$$

We consider the linear and continuous operator $\mathcal{M}:\ell^2\to\ell^2$

$$\mathcal{M}[z_n]=\sum_{j=1}^{N}[z_{(n_1,n_2,\ldots,n_j+1,n_{j+1},\ldots,n_N)}+z_{(n_1,n_2,\ldots,n_j-1,n_{j+1},\ldots,n_N)}],$$

satisfying

$$\big\|\mathcal{M}[\phi]-\mathcal{M}[\psi]\big\|_2\leq 2N\|\phi-\psi\|,\quad\text{for all }\phi,\psi\in\ell^2.\tag{3.6}$$

Then, the first term of the right-hand side of (3.5) can be written as

$$\alpha\big(\mathcal{J}[\xi_n]-\mathcal{J}[\zeta_n]\big)=\alpha\mathcal{M}\big[|\xi_n|^2\big](\xi_n-\zeta_n)+\alpha\zeta_n\big(\mathcal{M}\big[|\xi_n|^2\big]-\mathcal{M}\big[|\zeta_n|^2\big]\big).$$

By using (3.6) and inequality (3.3) for $p=4$ and $q=2$, we observe that

$$\begin{aligned}\big\|\mathcal{M}\big[|\xi|^2\big](\xi-\zeta)\big\|_2^2 &= \sum_{n\in\mathbb{Z}^N}\mathcal{M}^2\big[|\xi_n|\big]|\xi_n-\zeta_n|^2\\ &\le \sup_{n\in\mathbb{Z}^N}\big|\mathcal{M}\big[|\xi_n|^2\big]\big|^2\sum_{n\in\mathbb{Z}^N}|\xi_n-\zeta_n|^2\\ &\le 4N^2\sum_{n\in\mathbb{Z}^N}|\xi_n|^4\sum_{n\in\mathbb{Z}^N}|\xi_n-\zeta_n|^2\\ &\le 4N^2\Big(\sum_{n\in\mathbb{Z}^N}|\xi_n|^2\Big)^2\sum_{n\in\mathbb{Z}^N}|\xi_n-\zeta_n|^2\\ &\le 4N^2R^4\|\xi-\zeta\|_2^2. \end{aligned}\tag{3.7}$$

Using again (3.7) we get

$$\begin{aligned}\big\|\zeta\big(\mathcal{M}\big[|\xi|^2\big]-\mathcal{M}\big[|\zeta|^2\big]\big)\big\|_2^2 &= \sum_{n\in\mathbb{Z}^N}|\zeta_n|^2\big|\mathcal{M}\big[|\xi_n|^2\big]-\mathcal{M}\big[|\zeta_n|^2\big]\big|^2\\ &\le 4N^2\sup_{n\in\mathbb{Z}^N}|\zeta_n|^2\sum_{n\in\mathbb{Z}^N}\big||\xi_n|^2-|\zeta_n|^2\big|\\ &\le 4N^2R^2\sup_{n\in\mathbb{Z}^N}\big(|\xi_n|+|\zeta_n|\big)^2\sum_{n\in\mathbb{Z}^N}|\xi_n-\zeta_n|^2\\ &\le 8N^2R^4\|\xi-\zeta\|_2^2. \end{aligned}\tag{3.8}$$

Hence, from (3.7) and (3.8), the inequality

$$\big\|\mathcal{J}[\xi]-\mathcal{J}[\zeta]\big\|_2\le\sqrt{12}NR^2\|\xi-\zeta\|_2\tag{3.9}$$

readily follows. Moreover, we have (cf. Cuevas et al. 2009, Lemma II.2)

$$\sum_{n\in\mathbb{Z}^N}\big||\zeta_n|^{2\sigma}\zeta_n-|\xi_n|^{2\sigma}\xi_n\big|^2\le(2\sigma+1)^2R^{4\sigma}\sum_{n\in\mathbb{Z}^N}|\zeta_n-\xi_n|^2.\tag{3.10}$$

Now, taking the scalar product of (3.5) with χ in ℓ^2 and using (3.9) and (3.10), we have

$$\begin{aligned}\epsilon(-\Delta_d\chi,\chi)_2+\Omega\|\chi\|_2^2 &\le \alpha\|\chi\|_2\big\|\mathcal{J}[\xi]-\mathcal{J}[\zeta]\big\|_2+\beta\|\chi\|_2\big\||\zeta|^{2\sigma}\zeta-|\xi|^{2\sigma}\xi\big\|_2\\ &\le L(R)\|\chi\|_2\|\zeta-\xi\|_2, \end{aligned}\tag{3.11}$$

where

$$L(R)=\sqrt{12}\alpha NR^2+\beta(2\sigma+1)R^{2\sigma}.$$

Since $(-\Delta_d\chi,\chi)_2\ge 0$, from (3.11) we get the inequality

$$\Omega\|\chi\|_2^2\le\frac{L^2(R)}{2\Omega}\|\zeta-\xi\|_2^2+\frac{\Omega}{2}\|\chi\|_2^2.\tag{3.12}$$

From (3.12), we conclude that

$$\|\chi\|_2^2 = \|\mathcal{A}(z) - \mathcal{A}(\xi)\|_2^2 \leq \frac{L^2(R)}{\Omega^2}\|\zeta - \xi\|_2^2,$$

and, hence, the map $\mathcal{A} : B_R \to B_R$ is Lipschitz continuous with the Lipschitz constant

$$M(R) = \frac{L(R)}{\Omega}.$$

The map $\mathcal{A}$ is a contraction, and hence, has a unique fixed point if

$$M(R) < 1. \tag{3.13}$$

This unique fixed point is the trivial one, since $\mathcal{A}(0) = 0$. We consider the polynomial function

$$\Pi(R) := L(R) - \Omega. \tag{3.14}$$

The threshold value for the existence of non-trivial breather solutions can be derived from condition (3.13), as in the proof of Theorem 2.3B: Denote by R_{crit} the positive root of the polynomial equation $\Pi(R) = 0$. Then $\Pi(R) < 0$ for every $R \in (0, R_{\text{crit}})$, that is, condition (3.13) is satisfied if $R \in (0, R_{\text{crit}})$. Therefore breathers of arbitrary energy do not exist. A breather should have power $R^2 > R_{\text{crit}}^2$. We summarize in

Theorem 3.1 *We assume that the parameters $\alpha, \beta, \sigma > 0$. Let $R_{\text{crit}} > 0$ denote the unique positive root of the polynomial equation $\Pi(R) = 0$, where $\Pi(R)$ is given by (3.14). Then a breather solution $\psi_n(t) = e^{i\Omega t}\phi_n$, for any $\Omega > 0$ of (1.1) must have power $\mathcal{P} > R_{\text{crit}}^2$.*

The simple geometric interpretation of Theorem 3.1 is visualized in Fig. 1. Breathers do not exist in the sphere $B(0, R_{\text{crit}})$ of the energy space ℓ^2.

3.2 Estimates for Supercritical Nonlinearity Exponents $\sigma \geq 2/N$

A different version of dimension-dependent estimates in the case of the infinite lattice can be produced by using the discrete interpolation inequality of Weinstein (1999)

$$\sum_{n\in\mathbb{Z}^N} |\phi_n|^{2\sigma+2} \leq C_* \left(\sum_{n\in\mathbb{Z}^N} |\phi_n|^2 \right)^{\sigma} (-\Delta_d\phi, \phi)_2, \quad \sigma \geq \frac{2}{N}. \tag{3.15}$$

However, since (3.15) is valid only for $\sigma \geq N/2$, *the derived estimates will refer only to this range of parameters*. We recall that the range $\sigma \geq N/2$ is related to the appearance of the excitation threshold for breathers on DNLS lattices with power law nonlinearity.

We start by multiplying (2.3) by ϕ and summing over $\mathbb{Z}^N$, to get the equation

$$\epsilon(-\Delta_d\phi, \phi)_2 + \Omega \sum_{n\in\mathbb{Z}^N} |\phi_n|^2 = \alpha \sum_{n\in\mathbb{Z}^N} \sum_{j=1}^{N} |\phi_n|^2 (\mathcal{T}_j\phi)_{n\in\mathbb{Z}^N} + \beta \sum_{n\in\mathbb{Z}^N} |\phi_n|^{2\sigma+2}. \tag{3.16}$$

Using (3.15) in order to estimate the $(-\Delta_d\phi, \phi)_2$ term of (3.16) we have

$$\frac{\epsilon}{C_*}\frac{\sum_{n\in\mathbb{Z}^N}|\phi_n|^{2\sigma+2}}{(\sum_{n\in\mathbb{Z}^N}|\phi_n|^2)^\sigma}+\Omega\sum_{n\in\mathbb{Z}^N}|\phi_n|^2$$
$$\le\alpha\sum_{n\in\mathbb{Z}^N}\sum_{j=1}^{N}|\phi_n|^2(\mathcal{T}_j\phi)_{n\in\mathbb{Z}^N}+\beta\sum_{n\in\mathbb{Z}^N}|\phi_n|^{2\sigma+2}$$
$$\le 2\alpha N\Big(\sum_{n\in\mathbb{Z}^N}|\phi_n|^2\Big)^2+\beta\sum_{n\in\mathbb{Z}^N}|\phi_n|^{2\sigma+2}. \tag{3.17}$$

The inequality (3.17) can be rewritten as

$$\Omega R^2\le 2\alpha N R^4+\Big(\beta-\frac{\epsilon}{C_*R^{2\sigma}}\Big)\sum_{n\in\mathbb{Z}^N}|\phi_n|^{2\sigma+2}. \tag{3.18}$$

By using (3.3), this time for $p=2\sigma+2$ and $q=2$, the term $\sum_{n\in\mathbb{Z}^N}|\phi_n|^{2\sigma+2}$ of (3.18) can be estimated in terms of the power $\sum_{n\in\mathbb{Z}^N}|\phi_n|^2=R^2$, as

$$\sum_{n\in\mathbb{Z}^N}|\phi_n|^{2\sigma+2}\le\Big(\sum_{n\in\mathbb{Z}^N}|\phi_n|^2\Big)^{\frac{2\sigma+2}{2}}=R^{2\sigma+2}.$$

Thus, from (3.18) and the above estimate, we derive that

$$\Omega R^2\le 2\alpha N R^4+\Big(\beta-\frac{\epsilon}{C_*R^{2\sigma}}\Big)R^{2\sigma+2},$$

implying that the power satisfies the inequality

$$\Big(\Omega+\frac{\epsilon}{C_*}\Big)\le 2\alpha N R^2+\beta R^{2\sigma}. \tag{3.19}$$

Theorem 3.2 *Assume that $\sigma\ge 2/N$ and the parameters $\alpha,\beta,\Omega>0$. Let $\hat{R}_{\rm crit}>0$ denote the unique positive root of the polynomial equation*

$$2\alpha N R^2+\beta R^{2\sigma}-\Big(\Omega+\frac{\epsilon}{C_*}\Big)=0.$$

Then a breather solution $\psi_n(t)=e^{{\rm i}\Omega t}\phi_n$, for any $\Omega>0$ of (1.1) must have power $\mathcal{P}>\hat{R}^2_{\rm crit}$.

For an even more explicit estimate, at least an estimation of the optimal constant C_* is needed. This is provided by

Proposition 3.3 *Let $\sigma\ge 2/N$. There exists $\nu_{\rm crit}>1/2$ such that the optimal constant of the inequality (3.15) satisfies*

$$\frac{1}{4N}<C_*<\frac{\nu_{\rm crit}}{\sqrt{2\nu_{\rm crit}-1}}\frac{2\sigma+1}{4N},\quad N\ge 1. \tag{3.20}$$

Proof One of the fundamental results of Weinstein (1999) is the characterization of the optimal constant C_* involving the *excitation threshold* for breathers of the focusing DNLS equation with power nonlinearity. For instance, it is known that

$$\mathcal{R}_{\text{thresh}} = \left[\frac{(\sigma+1)\epsilon}{C_*}\right]^{\frac{1}{\sigma}}.$$

On the other hand, it was proved in Cuevas et al. (2009, Proposition II.1, p. 6) that there exists $\nu_{\text{crit}} > 1/2$ such that

$$\left[\frac{\sqrt{2\nu_{\text{crit}}-1}}{\nu_{\text{crit}}}\cdot\frac{4N\epsilon(\sigma+1)}{2\sigma+1}\right]^{\frac{1}{\sigma}} < R_{\text{thresh}} < \left[4\epsilon N(\sigma+1)\right]^{\frac{1}{\sigma}}. \tag{3.21}$$

The estimate (3.20) follows by inserting the characterization for $\mathcal{R}_{\text{thresh}}$ into (3.21). □

Together with Proposition 3.3, Theorem 3.2 can be restated and refined as follows.

Theorem 3.4 *We assume that*

$$\sigma \geq 2 \quad \textit{when } N=1 \quad \textit{and} \quad \sigma > 1 \quad \textit{when } N \geq 2. \tag{3.22}$$

Then a breather solution of (1.1) *satisfies the lower bound*

$$\left[\frac{1}{2\beta}\left(\Omega + \frac{4\epsilon N}{2\sigma+1}\frac{\sqrt{2\nu_{\text{crit}}-1}}{\nu_{\text{crit}}} - \frac{(2\alpha N)^{\frac{\sigma}{\sigma-1}}}{(\beta\sigma)^{\frac{1}{\sigma-1}}}\frac{\sigma-1}{\sigma}\right)\right]^{\frac{1}{\sigma}} < R^2, \tag{3.23}$$

in either the cases:

(i) (*lattice spacing condition*) *For all* $\Omega > 0$ *if*

$$\epsilon > \frac{(2\alpha N)^{\frac{\sigma}{\sigma-1}}}{(\beta\sigma)^{\frac{1}{\sigma-1}}}\frac{(\sigma-1)(2\sigma+1)}{4N\sigma}\frac{\nu_{\text{crit}}}{\sqrt{2\nu_{\text{crit}}-1}}. \tag{3.24}$$

(ii) (*frequency condition*) *For all* $\epsilon > 0$ *if*

$$\Omega > \frac{(2\alpha N)^{\frac{\sigma}{\sigma-1}}}{(\beta\sigma)^{\frac{1}{\sigma-1}}}\frac{\sigma-1}{\sigma}. \tag{3.25}$$

Proof Inequality (3.19) can be strengthened from below by replacing $1/C^*$ by its lower estimate as indicated from (3.20). Then, (3.23) comes out exactly as in Theorem 2.3C. □

We remark that in the case of the limit $a = 0$, if we repeat the calculations leading to the energy equation (3.16) and inequalities (3.17)–(3.18), we derive the inequality

$$0 < \Omega R^2 \leq \left(\beta - \frac{\epsilon}{C_* R^{2\sigma}}\right)\sum_{n\in\mathbb{Z}^N}|\phi_n|^{2\sigma+2}. \tag{3.26}$$

Now, the positivity of the right-hand side of (3.26) implies that in the limit $\alpha = 0$, the Ω-independent lower bound

$$\left[\frac{\epsilon}{C_*\beta}\right]^{\frac{1}{\sigma}} < R^2$$

is satisfied.

Let us also remark that the non-existence result of Theorem 3.1 is valid in finite lattices, due to the validity of inequality (3.3) in the subspace $\ell^2(\mathbb{Z}_K^N)$ of $\ell^2(\mathbb{Z}^N)$. Thus, the result can be proved in the case of finite lattices without any additional implications. Similarly, inequality (3.15) is also valid in $\ell^2(\mathbb{Z}_K^N)$ and the estimates of Theorem 3.4 can be proved to be valid in finite lattices. The estimates of Theorem 3.4 for the case $\sigma \geq 2/N$, will be tested numerically in the next section where the unspecified parameter ν_{crit} will be also discussed.

4 Numerical Study

We present in this section, numerical results testing the behavior and relevance of the theoretical estimates, in the case of the 1D lattice. The structure of this section is as follows. In Sect. 4.1.1 we analyze theoretically a refinement of the original variational estimates on the example of the focusing case $\alpha, \beta > 0$, aiming to improve the capture of the contribution of the linear part of the system to the power. This contribution is manifested in the bounds, by the first eigenvalue of the discrete Laplacian. The refinement takes into account the localization of true breather solutions, by performing a "cut-off" procedure, focusing on the most excited states. The improvement is reflected in the numerical simulations performed in Sect. 4.1.2 for the case of the cubic nonlinearity $\sigma = 1$, showing in particular that in some cases of the weak coupling regime, the estimates provide an accurate prediction of the numerical power. In Sect. 4.1.3 we present the numerical results for the case of the quintic nonlinearity $\sigma = 2$. The refined variational estimates are valid, due to the translational invariance of the "cut-off" procedure, even in the case of the infinite lattices, and have been tested against the interpolation estimates (e.g. those by the interpolation inequality of Gagliardo–Nirenberg type). It was interesting to observe that the refined variational bounds give a better qualitative prediction when the nonlinearity parameter β is varied, while the interpolation estimates behave better for large values of frequencies Ω. Finally, in Sect. 4.2, we present an indicative numerical study of the interpolation estimates in the defocusing case $\alpha < 0$, $\beta < 0$. The main finding here is that the theoretical predictions are improved for large values of the parameters β and σ.

We note that in all the numerical simulations, the results have been obtained for a 1D-lattice of $K = 101$ particles.

4.1 Focusing Case ($\alpha > 0, \beta > 0$) with Dirichlet Boundary Conditions. Solutions $\psi_n(t) = e^{i\Omega t}\phi_n$, $\Omega > 0$

4.1.1 Theoretical Analysis of the "Cut-Off" Procedure

According to the results of Theorem 2.3A, without any restrictions on the exponent $\sigma > 0$ of the nonlinearity, the first lower bound comes from the positive root $R_{*,f}$ of (2.10):

$$\beta\chi^{2\sigma} + 2\alpha N\chi^2 - (\mu_1 + \Omega) = 0, \quad \sigma > 0, N \geq 1. \tag{4.1}$$

Then any breather solution has power $\mathcal{P}[\phi]$ satisfying the lower bound

$$R_{*,f}^2 < \mathcal{P}, \quad \text{for all } \sigma > 0,\ N \geq 1. \tag{4.2}$$

In the particular case of the *cubic nonlinearity* this lower bound reads

$$\frac{\mu_1 + \Omega}{2\alpha N + \beta} < \mathcal{P}, \quad \sigma = 1,\ N \geq 1. \tag{4.3}$$

Due to its relevance from a physical point of view, we have chosen the cubic nonlinearity for a first numerical test. The principal eigenvalue in (4.3) manifests the contribution of the linear part of (1.5). The variational characterization of the principal eigenvalue (1.22), shows that the contribution of the linear part to the real breather is estimated from below by the eigenvector ϕ^1 corresponding to the principal eigenvalue μ_1, since the infimum in (1.22) is attained by ϕ^1 as

$$\mu_1 = \frac{(-\epsilon\Delta_d\phi^1, \phi^1)_2}{\sum_{\|n\|\leq K} |\phi_n^1|^2}, \tag{4.4}$$

and (1.22) holds for all $\phi \in \ell^2(\mathbb{Z}_K^N)$. Qualitatively and geometrically, this approximation of the linear part seems reasonable, especially for breather solutions without sign changes (zero-crossings), since the eigenvector ϕ^1 has no sign changes. On the other hand, real numerical computations should consider a sufficiently large chain length L, especially when the infinite chain is modeled in order to avoid the influence of boundary conditions. In this case, $\mu_1 \to 0$ (see (1.15)–(1.20)) and the contribution of this approximation becomes negligible. This can be explained physically, taking into account the fact that the real breather solution has a localization length $L_{\text{loc}} \ll L$ while the eigenvector is extended through the entire chain length L. Proceeding further, since the contribution to the power outside the breather width L_{loc} is also negligible, we could "cut-off" the estimation procedure, estimating the power in L_{loc} and the contribution of the linear part by the principal eigenvalue $\mu_{1,L_{\text{loc}}}$ of (1.13) considered on L_{loc}. Practically, since the breather width L_{loc} is unknown, we may perform this "cut-off" procedure in an interval close to the interval of unit length $L = 1$, expecting that the main contribution to the power comes from the excited sites included in the unit interval. This is certainly true for breathers centered around the center of the interval $[-L, L]$ located at the site $n = \frac{(K+1)}{2}$. It should be remarked that a breather can be always centered around the principal site, especially in the infinite lattice due to the integer translation invariance therein.

For instance, we will consider the interval $U = [-\frac{1}{2}, \frac{1}{2}]$ together with the first neighbors adjacent to the points $-\frac{1}{2}$ and $\frac{1}{2}$. We assume that the breather configuration is described by the vector $\phi \in \mathbb{R}^{K+2}$

$$\phi = (\phi_0, \phi_1, \ldots, \phi_{K+1}), \quad \phi_0 = \phi_{K+1} = 0, \tag{4.5}$$

where $\phi_n := \phi(x_n)$, $x_n = -\frac{L}{2} + nh$, $n = 0, \ldots, K+1$. The number of oscillators located outside the piece of the chain of unit length $U = [-\frac{1}{2}, \frac{1}{2}]$ is

$$\theta = 2\left\lceil \frac{(\frac{L}{2} - \frac{1}{2})(K+1)}{L} \right\rceil, \tag{4.6}$$

where $\lceil x \rceil = \min\{n \in \mathbb{Z} \,|\, n \geq x\}$, $x \in \mathbb{R}$. Then the number of oscillators included in the unit interval U is

$$m = K + 2 - \theta. \tag{4.7}$$

We also assume that the neighbors adjacent to the end-points of U, are located at the sites k and $k+m+1$. Note that these neighbors coincide with the end-points of U only when $\frac{1}{h} \in \mathbb{N}$. The distance $y \geq 0$ of these neighbors to the end-points of U is given by

$$y = h - \frac{1-(m-1)h}{2}, \quad \text{if } \frac{1}{h} \notin \mathbb{N}, \tag{4.8}$$

$$y = 0, \quad \text{if } \frac{1}{h} \in \mathbb{N}. \tag{4.9}$$

We denote by U' the interval occupied by the m oscillators in U and the two neighbors adjacent to the end-points of U, i.e., containing $m+2$ oscillators. The length of U' is

$$L' = 1 + 2y. \tag{4.10}$$

We have the following.

Proposition 4.1 *Let $\epsilon > 0$, $N = \sigma = 1$. Then the power of the m oscillators included in the interval U*

$$\mathcal{P}_U = \sum_{n=k+1}^{k+m} |\phi_n|^2,$$

satisfies the estimate

$$\frac{4\epsilon \sin^2(\frac{\pi}{2(m+1)}) + \Omega}{2\alpha + \beta} < \mathcal{P}_U < \mathcal{P}, \tag{4.11}$$

where the number of points m in U is given by (4.7).

Proof The breather configuration vector ϕ in (4.5) can be decomposed as $\phi = \phi^{L\setminus U} + \phi^U$

$$\phi^{L\setminus U} = (\phi_0, \phi_1, \ldots, \phi_{k-1}, \phi_k, 0, \ldots, 0, \phi_{k+m+1}, \ldots, \phi_{K+2}), \tag{4.12}$$

$$\phi^U = (0, \ldots, 0, \phi_{k+1}, \phi_{k+2}, \ldots, \phi_{k+m}, 0 \ldots, 0). \tag{4.13}$$

Since the decomposition is linear, at first glance the elements $\phi^{L\setminus U}$ and ϕ^U satisfy the equations

$$\begin{aligned}
&-\epsilon \Delta_d \phi_n^U + \Omega \phi_n^U - \alpha \phi_n^U \left(|\phi_{n+1}|^2 + |\phi_{n-1}|^2\right) + \beta |\phi_n|^{2\sigma} \phi_n^U = 0,\\
&\quad n = 0, \ldots, K+2,\\
&-\epsilon \Delta \phi_n^{L\setminus U} + \Omega \phi_n^{L\setminus U} - \alpha \phi_n^{L\setminus U} \left(|\phi_{n+1}|^2 + |\phi_{n-1}|^2\right) + \beta |\phi_n|^{2\sigma} \phi_n^{L\setminus U} = 0,\\
&\quad n = 0, \ldots, K+2.
\end{aligned}$$

However, on the account of (4.13), the equation for ϕ_U can be written as

$$-\epsilon\Delta_d\phi_n^U + \Omega\phi_n^U - \alpha\phi_n^U\left(\left|\phi_{n+1}^U\right|^2 + \left|\phi_{n-1}^U\right|^2\right) + \beta\left|\phi_n^U\right|^{2\sigma}\phi_n^U = 0,$$
$$n = k+1, \ldots, k+m+1,$$
$$\phi_k^U = \phi_{k+m+1}^U = 0.$$

Relabeling for convenience, the system for ϕ^U can be considered on the interval U' of the $m+2$ oscillators $j = 0, \ldots, m+2$ as

$$-\epsilon\Delta_d\phi_j^U + \Omega\phi_j^U - \alpha\phi_j^U\left(\left|\phi_{j+1}^U\right|^2 + \left|\phi_{j-1}^U\right|^2\right) + \beta\left|\phi_j^U\right|^{2\sigma}\phi_j^U = 0, \quad j = 1, \ldots, m, \tag{4.14}$$

$$\phi_0^U = \phi_{m+1}^U = 0. \tag{4.15}$$

We also consider the linear eigenvalue problem on U'

$$-\epsilon\Delta_d\phi_j = \mu\phi_j, \quad j = 1, \ldots, m, \tag{4.16}$$

$$\phi_0 = \phi_{m+1} = 0. \tag{4.17}$$

The principal eigenvalue $\mu_{1,U'}$ of (4.16)–(4.17) is given by

$$\mu_{1,U'} = 4\epsilon\sin^2\left(\frac{\pi L'}{2L'(m+1)}\right) = 4\epsilon\sin^2\left(\frac{\pi}{2(m+1)}\right). \tag{4.18}$$

Repeating the calculations of the proof of Theorem 2.3 on the system (4.14)–(4.15), we derive that

$$\frac{\mu_{1,U'} + \Omega}{2\alpha + \beta} < \mathcal{P}_U < \mathcal{P}, \quad \sigma = 1, N \geq 1,$$

i.e., the left-hand side of (4.11). The left-hand side follows from the fact that $\mathcal{P} = \sum_{j=1}^{K+2}|\phi_j|^2 > P_U$. □

Remark 4.2 The estimate (4.11) will be useful for the numerical simulations, since it is valid for any ϵ and can be used for the fully discrete case, even in the case of an infinite lattice. This is so because the interval U' where the procedure takes place, is the same, independently of the length of the chain. Thus even in the case $h > 0.5$, where the unit interval U contains only the centered site, we may perform the "cut-off" procedure for the centered site and the two adjacent neighbors occupying the interval U' of length $L' = 1 + 2y = 1 + 2(h - \frac{1}{2})$. The estimate (4.11) reads

$$\frac{4\epsilon\sin^2(\frac{\pi}{4}) + \Omega}{2\alpha + \beta} < \mathcal{P}_U < \mathcal{P}, \tag{4.19}$$

estimating the power of the breather in terms of the "most excited site".

In the case we approximate the continuous limit by considering $\epsilon > 0$ sufficiently large, we have

Proposition 4.3 *Let $\epsilon \cong \frac{1}{h^2}$, $N = \sigma = 1$. Assume that ϵ is sufficiently large, or $\frac{1}{h} \in \mathbb{N}$. The power of the m oscillators included in the interval U,*

$$\mathcal{P}_U = \sum_{n=k+1}^{k+m} |\phi_n|^2,$$

satisfies

$$\frac{4(m+1)^2 \sin^2(\frac{\pi}{2(m+1)}) + \Omega}{2\alpha+\beta} < \mathcal{P}_U < \mathcal{P}, \tag{4.20}$$

where the number of points m in U is given by (4.7).

Proof Working as in the proof of Proposition 4.1, we estimate the linear part of (4.14)–(4.15), by using the principal eigenvalue of the linear problem (4.16)–(4.17), where in the case $\epsilon \cong \frac{1}{h^2}$, is

$$\mu_{1,U'} \cong \frac{4}{h'^2} \sin^2\left(\frac{\pi h'}{2L'}\right) = 4\frac{(m+1)^2}{(1+2y)^2} \sin^2\left(\frac{\pi}{2(m+1)}\right), \tag{4.21}$$

since the spacing of U' is

$$h' = \frac{L'}{m+1} = \frac{1+2y}{m+1}.$$

The distance y is defined in (4.8)–(4.9). Letting $h \to 0$ we have $y \to 0$ (not monotonically), and (4.21) implies that

$$\mu_{1,U'} \cong 4(m+1)^2 \sin^2\left(\frac{\pi}{2(m+1)}\right). \tag{4.22}$$

When $\frac{1}{h} \in \mathbb{N}$, the end-points of U' are $x_k = -1/2$ and $x_{k+m+1} = 1/2$, and $y = 0$. □

Remark 4.4 When we approximate the continuum by considering $\epsilon > 0$ sufficiently large, we observe that the principal eigenvalue $\mu_{1,U'}$ has the expression (1.15) for $L = 1$, in terms of the number $m+2$ of oscillators occupying the interval U'. Clearly, since $\frac{1}{m+1} < 1$ for $m \geq 1$

$$4 < \mu_{1,U'} = 4(m+1)^2 \sin^2\left(\frac{\pi}{2(m+1)}\right) < \pi^2, \tag{4.23}$$

and we have the bounds

$$\frac{4+\Omega}{2\alpha+\beta} < \frac{\mu_{1,U'}+\Omega}{2\alpha+\beta} < \mathcal{P}_U < \mathcal{P}. \tag{4.24}$$

Besides, for large $\epsilon > 0$, $m > 1$ is large enough and (4.23) and (4.24) justify the approximation

$$\mu_{1,U'} \sim 4\epsilon \sin^2\left(\frac{\pi}{2\sqrt{\epsilon}}\right),$$

and the estimation of the power as

$$\frac{4+\Omega}{2\alpha+\beta} < \frac{\mu_{1,U'}+\Omega}{2\alpha+\beta} < \mathcal{P}_U < \mathcal{P}, \quad \mu_{1,U'} \sim 4\epsilon \sin^2\left(\frac{\pi}{2\sqrt{\epsilon}}\right). \tag{4.25}$$

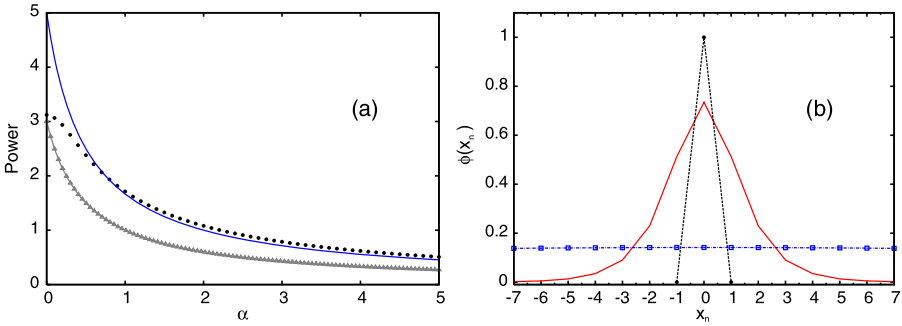

Fig. 2 (**a**) Power of breathers versus nonlinear parameter α in the HDNLS system with cubic nonlinearity ($\sigma = 1$) and $\epsilon = 1$. *Symbols* (*dots*) correspond to numerical calculations for the exact solutions while the *triangles* (*grey*) *line* represents estimation (4.19). The *continuous* (*blue*) *curve* corresponds to the estimate (4.25). Other parameters: $\beta = \Omega = 1$. (**b**) Breather profile (*continuous* (*red*) *curve*) against the eigenvector (*dashed* (*black*) *curve*) of (4.16)–(4.17) on the interval U' of length $L' = 2$. The eigenvector of (1.13) in the length L of the chain is represented by the *dashed-boxes* (*blue*) *curve* (Color figure online)

4.1.2 Numerical Results: Cubic Nonlinearity $\sigma = 1$

We now turn to the presentation of the numerical results which starts with the case $\epsilon = 1$. The "cut-off" approximation of Proposition 4.1 takes place on the interval U' of length $L' = 2$ ($y = 0.5$) and the unit interval U contains only one site ($m = 1$). In Fig. 2(a), the real power of a breather family is plotted using dots against the nonlinear parameter α. The lower bound obtained with the "cut-off" procedure (4.19) is shown with a triangle (grey) line. Notice that it is always below the real power. The qualitative prediction of the pattern of the numerical power as given by the theoretical estimate should be remarked, due to the effective approximation of the contribution of the linear and the nonlinear part to the power.

The continuous approximation (4.25) in the unit length, plotted with a continuous blue curve, is not satisfied as a lower bound for all the values of the parameter α as expected, since we are fairly far from the continuum limit. Remarkably, however, we observe that for a quite large regime of the parameter α, the corresponding prediction is below the numerical power. This is due to the fact that $\epsilon = 1$ is a critical value for our approximation in the sense that for $\epsilon = 1$ the eigenvalue $\mu_{1,U'}$ in (4.25) attains its minimum $\mu_{1,U'} = 4$.

In Fig. 2(b) the breather profile (continuous (red) curve) is plotted against the eigenvector on U' and the eigenvector on the length of the chain L for $\epsilon = \Omega = 1$ and $\beta = 2$. Notice that the eigenvector in the length of the system L is spread out along the chain (on the scale of the figure it is almost a horizontal line) and its contribution to the estimates would be negligible.

In Fig. 3 we present the results of the study for $\epsilon = 2$. Triangles (grey curve) correspond again to the estimate (4.19), still valid in the interval U' having now length $L' \sim 1.414$ and the unit interval U contains one site ($m = 1$). We observe the increased quantitative accuracy of the prediction of the actual power (symbols (dots)). The continuous approximation (4.25) in the unit length represented by the dash-dotted (blue) curve is not satisfied as a lower bound as predicted by Propositions 4.1

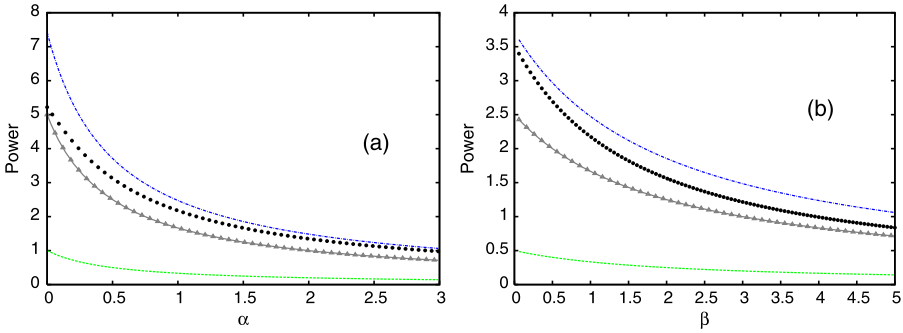

Fig. 3 (**a**) Power of breathers versus nonlinear parameter α in the HDNLS system with cubic nonlinearity ($\sigma = 1$) and $\epsilon = 2$. *Symbols* (*dots*) correspond to numerical calculations while the *triangles* (*grey*) *line* represents estimation (4.19) obtained with the "cut-off" approximation of Proposition 4.1. The *dash-dotted* (*blue*) *curve* corresponds to the continuous approximation (4.25). The first *dotted* (*green*) *curve* from below represents the initial estimate (4.3) with the eigenvalue μ_1 calculated over the length L of the system. Other parameters: $\beta = \Omega = 1$. (**b**) The power and its estimates versus the nonlinear parameter β. Other parameters are chosen as $\alpha = \Omega = 1$ (Color figure online)

and 4.3. Nevertheless, it is worth observing that the continuous approximation is only slightly above the actual value. This is connected to the fact that increasing values of ϵ correspond to a closer approximation of the continuous limit. The dotted (green) curve below the triangles represents the initial estimate (4.3) with the eigenvalue μ_1 corresponding to the eigenvector of (1.13) over the original length L of the system. In this case, the estimation of the contribution of the linear part to the power is negligible as (1.20) shows, thus (4.3) is well below the actual power.

The effectiveness of the "cut-off" approximation of Proposition 4.1 and Remark 4.2 on length L', if compared with the initial estimate (4.3) on the length of the system L is even more transparent in the study for $\epsilon = 3$, where the results are presented in Fig. 4. In this case $L' \sim 1.154$ and still $m = 1$. The curves are traced as in Fig. 3, except the new continuous (red) curve which is above the theoretical estimate (4.3). This curve corresponds to the lower bound in the left-hand side of (4.25). We observe that the prediction of (4.19) is of excellent accuracy throughout the continuation over the nonlinear parameter α and of very good accuracy even versus the nonlinear parameter β, being saturated for large values of β. It seems that the theoretical estimates capture better the variation over the nonlinear coupling coefficient α rather than the onsite nonlinearity coefficient β. This is due to the fact that through the estimation process of Theorem 2.3 the contribution of the hopping nonlinearity is "doubled" by the nonlinear coupling with the adjacent sites (see the inequality (2.22)), although both nonlinearities are of cubic order in the case $\sigma = 1$. For large values of β the manifestation of the power nonlinearity is stronger. More precisely, observe in Fig. 4(b) that the convergence of (4.19) to the real power starts after $\beta \geq 2$, i.e. after "doubling" the strength of the onsite nonlinearity. In this case, the continuous approximation over the unit length approaches further the actual power (still, however, from above).

The approximation procedure considers the cases $\epsilon = 1, 2, 3, 4$, as weak coupling cases, in the sense that the unit length U contains only one point and the spacing

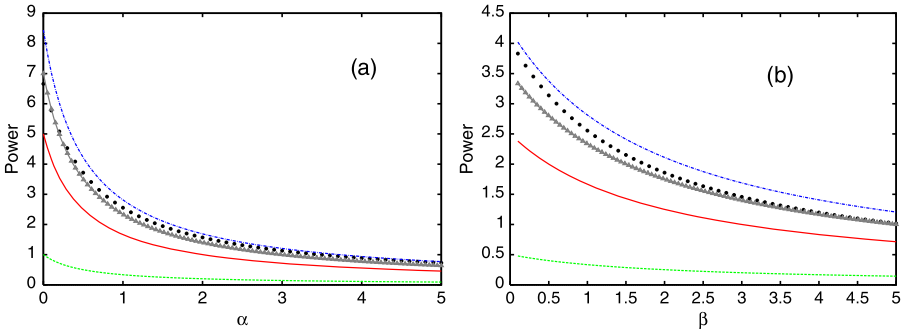

Fig. 4 (**a**) Power of breathers versus the nonlinear parameter α in the DNLS system with cubic nonlinearity ($\sigma = 1$) and $\epsilon = 3$. *Symbols* (*dots*) correspond to numerical calculations while the *triangles* (*grey*) *line* represents estimation (4.19) obtained with the "cut-off" approximation of Proposition 4.1. The *dash–dotted* (*blue*) *curve* corresponds to the continuous approximation (4.25). The first *dotted* (*green*) *curve* from below represents the initial estimate (4.3) with the eigenvalue μ_1 calculated over the length L of the system. Other parameters are chosen as $\beta = \Omega = 1$. (**b**) The power and its estimates versus the nonlinear parameter β. Other parameters are $\alpha = \Omega = 1$ (Color figure online)

is $h > 0.5$. Note that U' has a different length ($L' = 2$ for $\epsilon = 1$, $L' \sim 1.414$ for $\epsilon = 2$, $L' \sim 1.154$ for $\epsilon = 3$ and $L' = 1$ for $\epsilon = 4$). Since $m = 1$, the eigenvalue in U' given in (4.18) is always $\mu_{1,U'} = 2\epsilon$. Thus, in the weak coupling case, the continuous approximation in the unit length (4.25) is not valid and (4.25) is not satisfied as a lower bound for the power. On the other hand, the discrete approximation with the cut-off procedure within (4.19) becomes progressively better as ϵ is increased.

Propositions 4.1 and 4.3 predict that the position of the curves (4.19) and (4.25) should be interchanged when $\epsilon > 4$ ($h < 0.5$). In this case, the unit interval U contains more than one site ($m > 1$) and (4.19) is not valid. In Fig. 5 we present the numerical study for $\epsilon = 10$. Here U' has length $L' \sim 1.264$, the unit interval U contains three sites ($m = 3$) and $h \sim 0.316$, which can be considered as gradually approaching the continuous limit. Note that for $\epsilon > 4$ we have $L' \geq 1$; however, $y \to 0$ as ϵ is increased. We observe that (4.19) is well above the actual breather power in this case, while now (4.25) provides an adequate approximation especially versus the hopping parameter α.

Figures 2(b) and 6(a)–(b) are showing the breather profiles versus the eigenvectors on U' and the length L of the system, and demonstrate the main features of the approximation procedure. A first important feature is that both the real breather and the approximating eigenvector for the linear part contribution on U' are localized. This is in contrast to the eigenvector associated with μ_1 (of the original problem) which is extended over the entire length L of the system. This approximation of the linear part is effective for values of the weak coupling, where the eigenvector on U' has a width comparable with the localization length of the breather. In the anticontinuous limit, we expect strong localization effects while the eigenvalue $\mu_{1,U'} = 2\epsilon$ becomes negligible again, and the estimates are less effective.

The second feature is that although we are calculating only the contribution to the energy of the sites included in U', the approximation is focusing on these sites being the principal excited ones. Furthermore, Figs. 2(b) and 6(a), (b) demonstrate a

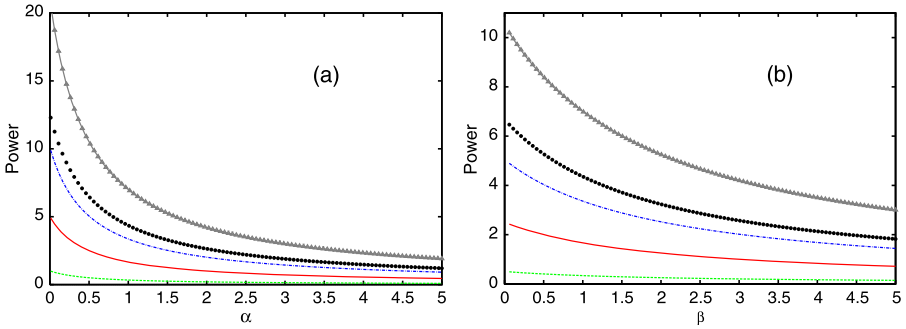

Fig. 5 (**a**) Power of breathers versus nonlinear parameter α in the HDNLS system with cubic nonlinearity ($\sigma = 1$) and $\epsilon = 10$. *Symbols* (*dots*) correspond to numerical calculations while the *triangles* (*grey*) *line* represents estimation (4.19) obtained with the "cut-off" approximation of Proposition 4.1. The *dotted-dashed* (*blue*) *curve* corresponds to the estimate (4.25). The first *dotted* (*green*) *curve* from below represents the initial estimate (4.3) with the eigenvalue μ_1 calculated in the length L of the system and the *continuous* (*red*) *curve* above stands for the estimate (4.25) with the lower bound $4\epsilon \leq \mu_1(\epsilon)$. Other parameters are chosen as $\beta = \Omega = 1$. (**b**) The power and its estimates are shown versus the nonlinear parameter β. Other parameters $\alpha = \Omega = 1$ (Color figure online)

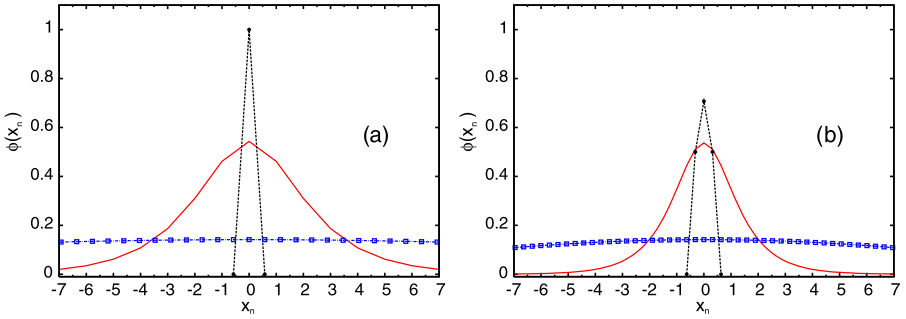

Fig. 6 (**a**) Breather profile for $\epsilon = 3$ (*continuous* (*red*) *curve*) against the eigenvector (*dashed* (*black*) *curve*) of (4.16)–(4.17) on the interval U' of length $L' \sim 1.154$. The eigenvector of (1.13) in the length L of the chain is represented by the *dashed-boxes* (*blue*) *curve*. Other parameters are $\alpha = 1$, $\beta = 5$, $\Omega = 1$. (**b**) Breather profiles for $\epsilon = 10$. Here $L' \sim 1.264$. Other parameters $\alpha = 1$, $\beta = 5$, $\Omega = 1$ (Color figure online)

concentration of the "missing" power of the sites outside U' to the most excited sites within the eigenvector on U'. This is observable by a comparison of the profiles for $\epsilon = 2, 3, 10$. From the strong coupling to the anticontinuous limit, the breather profile approaches the continuous one, while the eigenvector in U' converges to the continuous eigenfunction. Then, both the difference between the breather and the eigenvector width as well the difference of their "peaks" becomes constant, and again, the estimates are becoming less effective. Besides, the methods of this paper are making use of the properties of the discrete phase space and should be extended appropriately in function spaces in order to capture effectively the behavior of the continuous counterpart. Nevertheless, in this setting of larger ϵ, the continuum variant of the approximation over the interval U' yields a suitable lower threshold for the breather power.

4.1.3 Numerical Results: Quintic Nonlinearity $\sigma = 2$

Concerning the case of non-cubic nonlinearity ($\sigma \neq 1$), an explicit estimate from (4.2) comes out:

$$\left[\frac{1}{2\beta}\left(\Omega + \mu_1 - \frac{(2\alpha N)^{\frac{\sigma}{\sigma-1}}}{(\beta\sigma)^{\frac{1}{\sigma-1}}}\frac{\sigma-1}{\sigma}\right)\right]^{\frac{1}{\sigma}} < \mathcal{P}, \quad \sigma > 1, N \geq 1, \tag{4.26}$$

with some restriction on the parameters σ, Ω and ϵ given in Theorem 2.3C:

(i) for all $\Omega > 0$ if

$$\epsilon > \frac{(2\alpha N)^{\frac{\sigma}{\sigma-1}}}{(\beta\sigma)^{\frac{1}{\sigma-1}}}\frac{\sigma-1}{\lambda_1\sigma}, \quad \sigma > 1, N \geq 1, \tag{4.27}$$

and (ii) for all $\epsilon > 0$ if

$$\Omega > \frac{(2\alpha N)^{\frac{\sigma}{\sigma-1}}}{(\beta\sigma)^{\frac{1}{\sigma-1}}}\frac{\sigma-1}{\sigma}, \quad \sigma > 1, N \geq 1. \tag{4.28}$$

In the non-cubic case, the cut-off approximation of Proposition 4.1 leads to

Corollary 4.5 *Let $\sigma > 1$, $N = 1$. Then the estimate (4.26) is valid with μ_1 replaced by*

A. $\mu_{1,U'} = 4\epsilon \sin^2(\frac{\pi}{2(m+1)})$ *for any* $\epsilon > 0$.

B. $\mu_{1,U'} \sim 4\epsilon \sin^2(\frac{\pi}{2\sqrt{\epsilon}})$ *when* $\epsilon > 0$ *is sufficiently large.*

The theoretical estimates proposed in Sect. 3 for infinite lattices can also be used. While an infinite lattice cannot be modeled numerically, the estimates of Sect. 3 can serve as alternatives to those summarized above for the finite lattice. The unspecified parameter ν_{crit} involved in (3.21), in the estimate (3.23) and restrictions (3.24)–(3.25) has been determined by justified heuristic (and rigorous in the case of "large" σ) arguments in Cuevas et al. (2009, Sect. III, p. 7). For instance it was revealed that the value $\nu_{\text{crit}} = 1$ is valid for all $N \geq 1$ and $\sigma \geq 1$. Furthermore, this value is of very good accuracy for $N = 2$ and excellent for $N = 3$. Let us also recall that this value covers when $\sigma \in \mathbb{N}$, the cases which are of main physical interest (see also Dorignac et al. 2008 considering integer values of $\sigma \geq 2/N$).

For $\nu_{\text{crit}} = 1$, Theorem 3.2 predicts that for supercritical nonlinearity $\sigma \geq 2/N$ any breather solution must have power

$$\hat{R}^2_{\text{crit}} < \mathcal{P}. \tag{4.29}$$

$\hat{R}_{\text{crit}}$ is the positive root of the equation

$$2\alpha N R^2 + \beta R^{2\sigma} - \left(\Omega + \frac{4\epsilon N}{2\sigma+1}\right) = 0. \tag{4.30}$$

Theorem 3.4 gives explicitly

$$\left[\frac{1}{2\beta}\left(\Omega+\frac{4\epsilon N}{2\sigma+1}-\frac{(2\alpha N)^{\frac{\sigma}{\sigma-1}}}{(\beta\sigma)^{\frac{1}{\sigma-1}}}\frac{\sigma-1}{\sigma}\right)\right]^{\frac{1}{\sigma}}<R^2,$$
$$\sigma\geq 2 \text{ when } N=1 \text{ and } \sigma>1 \text{ when } N\geq 2, \tag{4.31}$$

in either of the cases below:

(i) for all $\Omega>0$ and lattice spacing satisfying

$$\epsilon>\frac{(2\alpha N)^{\frac{\sigma}{\sigma-1}}}{(\beta\sigma)^{\frac{1}{\sigma-1}}}\frac{(\sigma-1)(2\sigma+1)}{4N\sigma},$$
$$\sigma\geq 2 \text{ when } N=1 \text{ and } \sigma>1 \text{ when } N\geq 2, \tag{4.32}$$

and

(ii) for all $\epsilon>0$ and frequencies

$$\Omega>\frac{(2\alpha N)^{\frac{\sigma}{\sigma-1}}}{(\beta\sigma)^{\frac{1}{\sigma-1}}}\frac{\sigma-1}{\sigma},$$
$$\sigma\geq 2 \text{ when } N=1 \text{ and } \sigma>1 \text{ when } N\geq 2. \tag{4.33}$$

Additionally other choices of the parameter $\hat{\epsilon}$ in Young's inequality trick (see Theorem 2.3C), give versions of the estimates valid with different restrictions on the coupling parameter ϵ or the frequency Ω. Together with the choice used in Theorem 2.3C, another interesting one is the standard $\hat{\epsilon}=1$ corresponding to the version of (3.23),

$$\left[\frac{\sigma}{\sigma\beta+1}\left(\Omega+\frac{4\epsilon N}{2\sigma+1}-\frac{(\sigma-1)(2\alpha N)^{\frac{\sigma}{\sigma-1}}}{\sigma}\right)\right]^{\frac{1}{\sigma}}<R^2,$$
$$\sigma\geq 2 \text{ when } N=1 \text{ and } \sigma>1 \text{ when } N\geq 2. \tag{4.34}$$

The estimate (4.34) is valid

(i) for all $\Omega>0$ and lattice spacing satisfying

$$\epsilon>\frac{(2\alpha N)^{\frac{\sigma}{\sigma-1}}(\sigma-1)(2\sigma+1)}{4N\sigma},\quad \sigma\geq 2 \text{ when } N=1 \text{ and } \sigma>1 \text{ when } N\geq 2, \tag{4.35}$$

and in the case

(ii) for all $\epsilon>0$ and frequencies

$$\Omega>\frac{(2\alpha N)^{\frac{\sigma}{\sigma-1}}(\sigma-1)}{\sigma},\quad \sigma\geq 2 \text{ when } N=1 \text{ and } \sigma>1 \text{ when } N\geq 2. \tag{4.36}$$

Regarding the quintic nonlinearity, more specifically, we have performed a test of the estimates (4.26), (4.31) and (4.34) by fixing $\sigma=2$, and $\epsilon=1$. With these choices, restrictions (4.28)–(4.33) and (4.36) reduce to the very simple conditions $\Omega>\alpha^2/\beta$ and $\Omega>2\alpha^2$. We expect all the estimates to be satisfied as thresholds due to the increased strength of the power nonlinearity absorbing the contribution of the linear part, even in the case of (4.26)-B of Corollary 4.5, which is not justified theoretically. In Fig. 7(a) we have plotted the estimate (4.26)-A of Corollary 4.5, with triangles

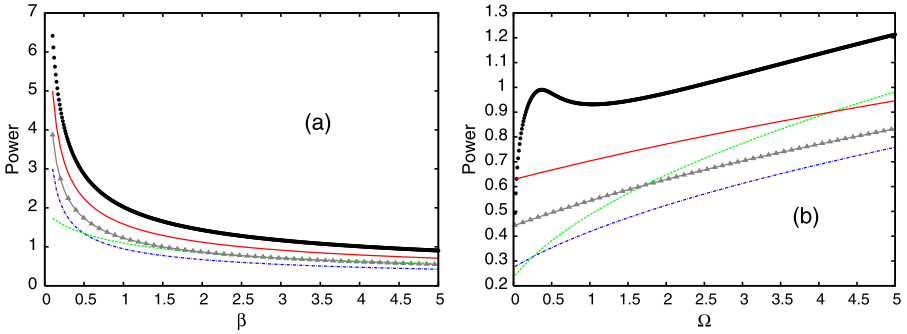

Fig. 7 (**a**) Power of breathers versus parameter β for supercritical nonlinearity $\sigma = 2$ in the HDNLS system. *Symbols* correspond to numerical calculations, the *dash-dotted* (*blue*) *line* represents estimation (4.31) and the *dashed line* (*green*) estimation (4.34). The estimate (4.26)-A of Corollary 4.5 corresponds to the *triangles* (*grey line*), and the estimate (4.26)-B with the *continuous* (*red*) *line*. Parameters: $\alpha = 0.01$, $\Omega = \epsilon = 1$. (**b**) Power versus frequency Ω for supercritical nonlinearity $\sigma = 2$. Parameters: $\alpha = 0.5$, $\beta = 5$ and $\epsilon = 1$ (Color figure online)

(grey curve), and its case B with the continuous (red) curve. The dash-dotted (blue) and dashed (green) lines correspond to (4.31) and (4.34), respectively. The numerical power (symbols) was obtained varying β for a small hopping parameter $\alpha = 0.01$ and $\Omega = 1$. Note that all the estimates are good, although (4.34) is better than (4.31) for large β while (4.31) behaves better when $\beta < 1/\sigma$.

In Fig. 7(b) we have plotted the breather power against Ω choosing $\beta = 5$ and $\alpha = 0.5$. Condition (4.28) is fulfilled for $\Omega > 0.05$ and condition (4.36) is fulfilled for $\Omega > 0.5$. In the latter region, since β is quite large, the estimate (4.34) behaves clearly better than (4.31). It is interesting to realize that (4.26) is worse than (4.34) for large enough frequencies.

4.2 Defocusing Case ($\alpha, \beta < 0$) with Dirichlet Boundary Conditions. Solutions $\psi_n(t) = e^{-i\Omega t}\phi_n$, $\Omega > 0$

In the defocusing case the results on the theoretical estimates are restricted to frequencies $\Omega > 4N\epsilon$. In this case, setting for convenience $\kappa = -\alpha > 0, \lambda = -\beta > 0$, the results of Theorem 2.5 state that for all $\sigma > 0$ the lower bound for the power of the staggered breathers is given by the positive root $R_{*,d}$ of the equation

$$\lambda\chi^{2\sigma} + 2\kappa N\chi^2 - (\Omega - 4\epsilon N) = 0, \quad \sigma > 0, N \geq 1, \Omega > 4\epsilon N, \tag{4.37}$$

and the power of staggered breathers satisfies

$$R_{*,d}^2 < \mathcal{P}, \quad \text{for all } \sigma > 0, N \geq 1, \Omega > 4\epsilon N. \tag{4.38}$$

In the defocusing case and *cubic nonlinearity*, the lower bound for the power is

$$\frac{\Omega - 4\epsilon N}{2\kappa N + \lambda} < \mathcal{P}, \quad \Omega > 4\epsilon N, N \geq 1, \sigma = 1. \tag{4.39}$$

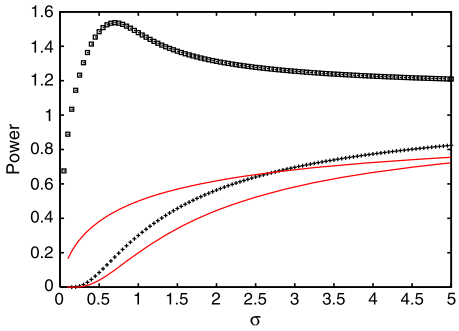

Fig. 8 Power of breathers versus parameter σ in the defocusing case. *Squares* (*pluses*) correspond to the numerical power found for $\beta = -1, \alpha = -0.5$ ($\beta = -5, \alpha = -0.01$), while the *upper* (*lower*) *continuous line* represents estimate (4.40). Other parameters: $\Omega = -2, \epsilon = 0.25$

The explicit estimate valid for $\sigma > 1$ is

$$\left[\frac{1}{2\lambda}\left(\Omega - 4\epsilon N - \frac{(2\kappa N)^{\frac{\sigma}{\sigma-1}}}{(\lambda\sigma)^{\frac{1}{\sigma-1}}}\frac{\sigma-1}{\sigma}\right)\right]^{\frac{1}{\sigma}} < \mathcal{P},$$

$$\sigma > 1, N \geq 1, \Omega > 4\epsilon N + \frac{(2\kappa N)^{\frac{\sigma}{\sigma-1}}}{(\lambda\sigma)^{\frac{1}{\sigma-1}}}\frac{\sigma-1}{\sigma}. \tag{4.40}$$

The results of the numerical tests in the defocusing case are similar to those of the focusing case and can be summarized in the following points:

- The theoretical estimates are always below the numerical power and approximate quite well the nonlinear part of the contribution to the power.
- The lower bound (4.38) is always above the explicit estimate (4.40).
- Estimate (4.40) behaves better for small values of the hopping parameter α and large exponents σ.

These observations are corroborated by the results of Fig. 8. Squares and the upper continuous curve correspond, respectively, to the numerical power and estimate (4.38) for $\beta = -1$ and a hopping parameter $\alpha = -0.5$. The estimate reaches values much closer to the real power when fixing $\beta = -5$ and $\alpha = -0.01$ (see pluses and the lower continuous curve).

5 Conclusions

In the present work, we generalized the considerations of energy thresholds in the setting of a DNLS model with generalized nonlinear (Hamiltonian) hopping terms. Different types of bounds were provided for the power both for finite and for infinite lattices, by using appropriate estimates for the linear coupling and nonlinear hopping terms. A fixed-point method establishing the contractivity of an appropriately defined operator was also used to establish that, for a given parameter set, there is a critical power, below which it is not possible to sustain such nonlinear waveforms. Finally, some dimension-dependent estimates were given based on the interpolation inequality of the Gagliardo–Nirenberg type, in a spirit similar to the work of Weinstein (1999).

Further improvements of the main theory have been considered and proved, appreciating the interplay of the nonlinear and linear term contributions within the true solitary wave solutions, taking into account their spatial localization. The obtained bounds were tested numerically and in all the cases where the theory was expected to be applicable, it was found that the numerical solutions satisfy the predicted norm inequalities. This aspect also provides details of the parameter regimes (weak linear coupling) which tend to saturate the corresponding theoretically obtained bounds.

We are leaving as an interesting open direction for a future work, to examine the behavior of the energy bounds when the size of the lattice is varied. This question is taking into account the effect of the transition from finite to infinite lattices, on the localization properties of the solutions. This task could be based on a generalization and use of the machinery developed in Penati and Paleari (2012), as well as of the relevant localization estimates. Such a generalization could be of particular interest in the case of multi-dimensional lattices.

It would be also interesting and relevant to examine how corresponding bounds can be generalized to other classes of models, including ones of the nonlinear Klein–Gordon or FPU type (or mixed ones), incorporating different types of onsite and intersite nonlinearity. Especially useful, albeit arguably more difficult, it is to extend the main strategy to continuous models. Such tasks will be considered in future publications.

Acknowledgements We are indebted to Chris Eilbeck for having suggested us to consider the model presented in the manuscript. B.S.R. and J.C. acknowledge financial support from the MICINN project FIS2008-04848. P.G.K. gratefully acknowledges support from the US National Science Foundation via grants NSF-DMS-0806762 and NSFCMMI-1000337, from the US Air Force via award FA9550-12-1-0332, as well as from the Alexander von Humboldt Foundation, the Alexander S. Onassis Public Benefit Foundation via grant RZG 003/2010-2011 and the Binational Science Foundation via grant 2010239.

References

Chow, S.N., Hale, J.K.: Methods of Bifurcation Theory. Grundlehren der mathematischen Wissenschaften—A series of Comprehensive Studies in Mathematics, vol. 251. Springer, New York (1982)

Christodoulides, D.N., Lederer, F., Silberberg, Y.: Discretizing light behavious in linear and nonlinear waveguide lattices. Nature **424**, 817–823 (2003)

Claude, Ch., Kivshar, Yu.S., Kluth, O., Spatschek, K.H.: Moving localized modes in nonlinear lattices. Phys. Rev. B **47**, 14228 (1993)

Cuevas, J., Eilbeck, J.C., Karachalios, N.I.: Thresholds for time periodic solutions on the discrete nonlinear Schrödinger equation with saturable and power nonlinearity. Discrete Contin. Dyn. Syst. **21**, 445–475 (2008a)

Cuevas, J., Eilbeck, J.C., Karachalios, N.: A lower bound for the power of periodic solutions of the defocusing discrete nonlinear Schrödinger equation. Dyn. Partial Differ. Equ. **5**, 69–85 (2008b)

Cuevas, J., Karachalios, N., Palmero, F.: Lower and upper estimates on the excitation threshold for breathers in discrete nonlinear Schrödinger lattices. J. Math. Phys. **50**, 112705 (2009)

Cuevas, J., Karachalios, N., Palmero, F.: Energy thresholds for the existence of breather solutions and traveling waves on lattices. Appl. Anal. **89**, 1351–1385 (2010)

Dorignac, J., Zhou, J., Campbell, D.K.: Discrete breathers in nonlinear Schrödinger hypercubic lattices with arbitrary power nonlinearity. Physica D **237**, 486–504 (2008)

Eilbeck, J.C., Johansson, M.: In: Vázquez, L., MacKay, R.S., Zorzano, M.P. (eds.) Localization and Energy Transfer in Nonlinear Systems, pp. 44–67. World Scientific, Singapore (2003)

Falvo, C., Pouthier, V., Eilbeck, J.C.: Fast energy transfer mediated by multi-quanta bound states in a nonlinear quantum lattice. Physica D **221**, 58–71 (2006)
Flach, S., Gorbach, A.V.: Discrete breathers—advances in theory and applications. Phys. Rep. **467**, 1–116 (2008)
Flach, S., Willis, C.R.: Discrete breathers. Phys. Rep. **295**, 181–264 (1998)
Flach, S., Kladko, K., MacKay, R.: Energy thresholds for discrete breathers in one-, two-, and three-dimensional lattices. Phys. Rev. Lett. **78**, 1207–1210 (1997)
Haskins, M., Speight, J.M.: Breather initial profiles in chains of weakly coupled anharmonic oscillators. Phys. Lett. A **299**, 549–557 (2002)
Hennig, D., Tsironis, G.: Wave transmission in nonlinear lattices. Phys. Rep. **307**, 333–432 (1999)
Herrmann, M.: Homoclinic standing waves in focusing DNLS equations. Discrete Contin. Dyn. Syst. **31**, 737–752 (2011)
Johansson, M.: Discrete nonlinear Schrödinger approximation of a mixed Klein–Gordon/Fermi–Pasta–Ulam chain: modulational instability and a statistical condition for creation of thermodynamic breathers. Physica D **216**, 62–70 (2006)
Karachalios, N.I.: A remark on the existence of breather solutions for the discrete nonlinear Schrödinger equation: the case of site dependent anharmonic parameter. Proc. Edinb. Math. Soc. **49**, 115–129 (2006)
Kastner, M.: Energy thresholds for discrete breathers. Phys. Rev. Lett. **92**(10), 104301 (2004)
Kevrekidis, P.G. (ed.): The Discrete Nonlinear Schrödinger Equation. Mathematical Analysis, Numerical Computations and Physical Perspectives. Springer, Berlin (2009)
Kevrekidis, P.G., Frantzeskakis, D.J.: Pattern forming dynamical instabilities of Bose–Einstein condensates. Mod. Phys. Lett. B **18**, 173–202 (2004)
Kevrekidis, P.G., Rasmussen, K.Ø., Bishop, A.R.: The discrete nonlinear Schrödinger equation: a survey of recent results. Int. J. Mod. Phys. B **15**, 2833–2900 (2001)
Kevrekidis, P.G., Susanto, H., Chen, Z.: High-order-mode soliton structures in two-dimensional lattices with defocusing nonlinearity. Phys. Rev. E **74**, 066606 (2006)
Kevrekidis, P.G., Frantzeskakis, D.J., Carretero-González, R. (eds.): Emergent Nonlinear Phenomena in Bose–Einstein Condensates: Theory and Experiment. Springer Series on Atomic, Optical, and Plasma Physics, vol. 45 (2008)
Kivshar, Y.S., Agrawal, G.P.: Optical Solitons: From Fibers to Photonic Crystals. Academic Press, San Diego (2003)
Konotop, V.V., Brazhnyi, V.A.: Theory of nonlinear matter waves in optical lattices. Mod. Phys. Lett. B **18**, 627–651 (2004)
Kundu, K.: Perturbative study of classical Ablowitz–Ladik type soliton dynamics in relation to energy transport in a-helical proteins. Phys. Rev. E **61**, 5839 (2000)
Lederer, F., Stegeman, G.I., Christodoulides, D.N., Assanto, G., Segev, M., Silberberg, Y.: Discrete solitons in optics. Phys. Rep. **463**, 1–126 (2008)
Morsch, O., Oberthaler, M.: Dynamics of Bose–Einstein condensates in optical lattices. Rev. Mod. Phys. **78**, 179–210 (2006)
Öster, M., Johansson, M.: Phase twisted modes and current reversals in a lattice model of waveguide arrays with nonlinear coupling. Phys. Rev. E **71**, 025601(R) (2005)
Öster, M., Johansson, M., Eriksson, A.: Enhanced mobility of strongly localized modes in waveguide arrays by inversion of stability. Phys. Rev. E **67**, 056606 (2003)
Öster, M., Gaididei, Y.B., Johansson, M., Christiansen, P.: Nonlocal and nonlinear dispersion in a nonlinear Schrödinger-type equation: exotic solitons and short-wavelength instabilities. Physica D **198**, 29–50 (2004)
Pelinovsky, D.E.: Translationally invariant nonlinear Schrödinger lattices. Nonlinearity **19**, 2695–2716 (2006)
Penati, T., Paleari, S.: Breathers and Q-Breathers: two sides of the same coin. SIAM J. Appl. Dyn. Syst. **11**, 1–30 (2012)
Peyrard, M.: Nonlinear dynamics and statistical physics of DNA. Nonlinearity **17**, R1–R40 (2004)
Sato, M., Hubbard, B.E., Sievers, A.J.: Nonlinear energy localization and its manipulation in micromechanical oscillator arrays. Rev. Mod. Phys. **78**, 137–157 (2006)
Weinstein, M.: Excitation thresholds for nonlinear localized modes on lattices. Nonlinearity **12**, 673–691 (1999)
Zeidler, E.: Linear Monotone Operators. Nonlinear Functional Analysis and Its Applications, vol. II/A. Springer, New York (1990)
Zeidler, E.: Applied Functional Analysis: Applications to Mathematical Physics. Applied Mathematical Sciences, vol. 108. Springer, New York (1995)